

## Review

# Central nervous system vascularization in human embryos and neural organoids

Sarah M. Boutom,<sup>1</sup> Teresa P. Silva,<sup>2,3,4</sup> Sean P. Palecek,<sup>5</sup> Eric V. Shusta,<sup>5,6</sup> Tiago G. Fernandes,<sup>2,3,\*</sup> and Randolph S. Ashton<sup>1,7,\*</sup>

<sup>1</sup>Department of Biomedical Engineering, University of Wisconsin-Madison, Madison, WI, USA

<sup>2</sup>Department of Bioengineering and IBB-Institute for Bioengineering and Biosciences, Instituto Superior Técnico, Universidade de Lisboa, Av. Rovisco Pais, 1049-001 Lisboa, Portugal

<sup>3</sup>Associate Laboratory i4HB-Institute for Health and Bioeconomy, Instituto Superior Técnico, Universidade de Lisboa, Av. Rovisco Pais, 1049-001 Lisboa, Portugal

<sup>4</sup>Instituto de Medicina Molecular João Lobo Antunes, Faculdade de Medicina, Universidade de Lisboa, Lisboa, Portugal

<sup>5</sup>Department of Chemical and Biological Engineering, University of Wisconsin-Madison, Madison, WI, USA

<sup>6</sup>Department of Neurological Surgery, University of Wisconsin School of Medicine and Public Health, Madison, WI, USA

<sup>7</sup>Wisconsin Institute for Discovery, University of Wisconsin-Madison, Madison, WI, USA

\*Correspondence: [tfernandes@tecnico.ulisboa.pt](mailto:tfernandes@tecnico.ulisboa.pt) (T.G.F.), [rashton2@wisc.edu](mailto:rashton2@wisc.edu) (R.S.A.)

<https://doi.org/10.1016/j.celrep.2024.115068>

## SUMMARY

In recent years, neural organoids derived from human pluripotent stem cells (hPSCs) have offered a transformative pre-clinical platform for understanding central nervous system (CNS) development, disease, drug effects, and toxicology. CNS vasculature plays an important role in all these scenarios; however, most published studies describe CNS organoids that lack a functional vasculature or demonstrate rudimentary incorporation of endothelial cells or blood vessel networks. Here, we review the existing knowledge of vascularization during the development of different CNS regions, including the brain, spinal cord, and retina, and compare it to vascularized CNS organoid models. We highlight several areas of contrast where further bioengineering innovation is needed and discuss potential applications of vascularized neural organoids in modeling human CNS development, physiology, and disease.

## VASCULARIZATION DURING HUMAN NEURAL TUBE MORPHOGENESIS

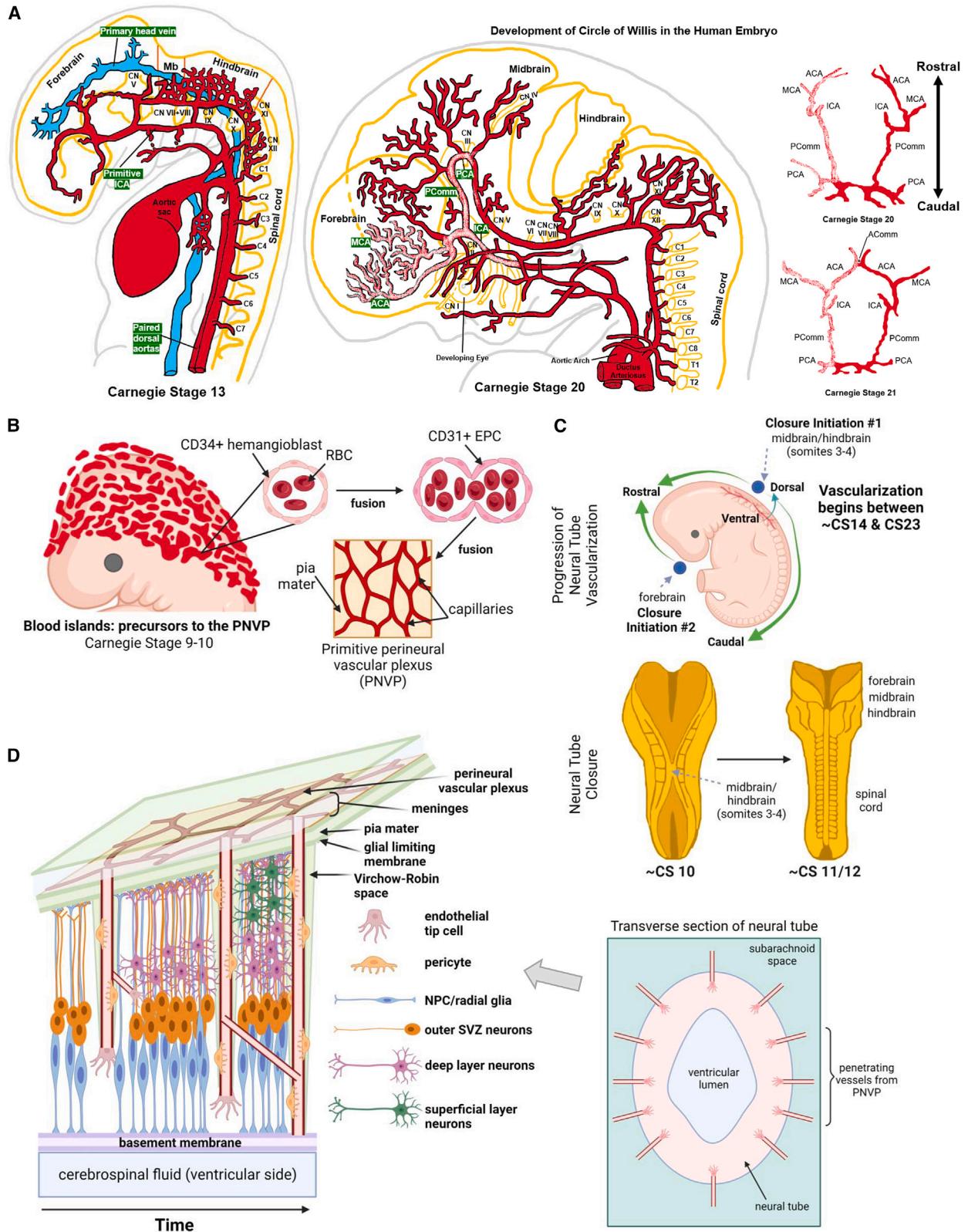
### Spatiotemporal progression of neural tube vascularization

In the embryo, human cranial vasculature (Figure 1A, left) begins forming ~21 days post-fertilization (~Carnegie stage [CS] 9), which is prior to primordial heart tube beating (~22/23 days) and initiation of neural tube closure (~CS 10/11). By CS 10, the dorsal aortas have formed and extend along the embryo from the developing primitive forebrain to the elongating posterior CNS, i.e., hindbrain and spinal cord, producing segmental branches at each somite.<sup>1</sup> By CS 13 (~30 days), there is a singular vein at the ventral midline of the developing brain called the vena capitis medialis, also known as (a.k.a.) the primary head vein, which eventually bifurcates into two major head veins that form the primitive cranial sinuses and drain into the anterior cardinal vein.<sup>2</sup> Simultaneously, the internal carotid arteries form from the dorsal aorta and bifurcate to form precursors of cranial and caudal portions of the circle of Willis (Figure 1A, right), an arterial anastomotic structure responsible for supplying blood to the brain.<sup>3</sup> By CS 21 (~52 days), all components of the circle of Willis can be readily distinguished.<sup>1,4</sup> Thus, approximate with the earliest stages of avascular neural tube development, the surrounding cerebral arterial and venous structures are already

being established. A more detailed description of human cranial artery development, from Streeter, Congdon, and Padgett's observations of Carnegie collection embryos, has been elegantly summarized in a recent review by Bertulli and Robert.<sup>1</sup>

Concurrent with the formation of major cranial arterial and venous structures, the development of the perineural vascular plexus (PNVP), a.k.a. pial capillary anastomotic plexus, initiates within the meningeal compartment, i.e., superficial to the neural tube's pial surface, between the 2<sup>nd</sup> (~CS 6) and 4<sup>th</sup> (~CS 10) gestational week (GWs).<sup>6–8</sup> After ~CS 9/10, PNVP formation is induced by vascular endothelial growth factor (VEGF)-A gradients emanating from the developing neural tube.<sup>9</sup> CD34<sup>+</sup> hemangioblasts migrate from mesodermal compartments toward the developing CNS and form “blood islands” (Figure 1B). Within these islands, they continue to differentiate into CD31<sup>+</sup> endothelial progenitors and undergo fusion to form the primitive PNVP.<sup>10</sup> Quail-chick and mouse-quail chimera studies of CNS vasculature indicate that endothelial cells (ECs) are incorporated into the PNVP by vasculogenesis.<sup>9</sup> However, more recent three-dimensional (3D) analysis of mouse embryonic vasculature via optical projection tomography suggests that the PNVP arises through a combination of vasculogenesis and angiogenic remodeling of existing vasculature in both the head and trunk regions.<sup>11</sup> By ~CS 17, the anterior, middle, and posterior meningeal plexuses have formed; the anterior plexus is associated





(legend on next page)

with the developing forebrain, middle plexus with the midbrain, and posterior plexus with the hindbrain.

The timing of PNVP invasion of the neural tube is debated and depends on the rostral-caudal or dorsal-ventral region being referenced. Along the rostral-caudal axis, the timing of neural tube closure slightly precedes that region's vascularization. Neural tube closure initiates primarily from a single point at the interface between the midbrain and hindbrain (near somites 3 and 4) and secondarily from a putative closure initiation point in the rostral forebrain<sup>12</sup> (Figure 1C). Light and electron microscopy studies of human embryos suggest that microvasculature is present within the neural tube as early as the 5<sup>th</sup> gestational week (GW; ~CS 14/15). Angiogenesis begins first in caudal portions of the midbrain and brainstem and progresses rostrally to include cortical vascular invasion by the ~6<sup>th</sup>–7<sup>th</sup> GW (~CS 17–19/20).<sup>2,13</sup> This timing appears to conflict with the analysis of human prosencephalic histologic sections prepared using the Golgi staining method. In these sections, microvascularization was not observed until the 8<sup>th</sup> GW (~CS 22/23), corresponding with dorsal forebrain cortical plate formation as indicated by the presence of CTIP2<sup>+</sup> pyramidal neurons and after the generation of apically oriented TBR1<sup>+</sup> neuronal pre-plate and basally positioned Reelin<sup>+</sup> Cajal-Retzius cells.<sup>8,14</sup> However, the disagreement may be because PNVP invasion initiates in ventral aspects of the neural tube prior to proceeding to dorsal regions.<sup>15</sup> Thus, the global progression of neural tube vascularization corresponds spatially with neural tube closure and development. Along the dorsal-ventral neuraxis, PNVP invasion proceeds from ventral to dorsal regions. Along the rostral-caudal neuraxis, vascularization proceeds from the mesencephalon (midbrain) and metencephalon (hindbrain) rostrally to the diencephalon and telencephalon (forebrain) as well as caudally through the myelencephalon and spinal cord (Figure 1C). This progression is supported by previous studies conducted by Klosovskii, Strong, Gamble, Bär and Wolff, and others in mouse, rat, rabbit, and human embryos.<sup>8,16</sup>

The neural tube's pial boundary, a.k.a. the external glial limiting membrane (EGLM), is composed of basal lamina secreted from

radial glia endfeet and separates the PNVP from neural tube tissue.<sup>8</sup> Vascularization by the PNVP initiates via fusion of capillary vascular and pial glial laminae followed by EGLM perforation by filopodia from capillary ECs (Figure 1D, right). The capillaries proceed to invade the neural parenchyma, growing radially via sprouting angiogenesis along a VEGF gradient.<sup>17</sup> As angiogenesis is initiated, these vessels begin to acquire properties such as selective regulation of solute transport and expression of intercellular junctions traditionally associated with the blood-brain barrier (BBB).<sup>18–20</sup> They grow into the neural tissue along the paths of radially oriented neural progenitors and radial glial cells<sup>21,22</sup> (Figure 1D, left). However, these vessels persist as an extrinsic structure via the presence of the circumferential Virchow-Robin compartment (V-RC), which remains open to the subarachnoid space indefinitely, serving as the precursor to the brain's perivascular glymphatic system.<sup>8,23</sup> Moreover, the intracerebral vascular smooth muscle cells/pericytes of the neural crest or mesodermal ontogeny enter the V-RC at the onset of vascularization.<sup>8,24–27</sup> These facets of CNS vascularization are often excluded from vascularized neural organoids despite forming simultaneously *in vivo*. Moreover, in addition to this section's general description of CNS vascularization, different neural tube regions have distinct nuances associated with their vascularization. Notable differences between forebrain, retina, midbrain, hindbrain, spinal cord, and choroid plexus (ChP) vascularization will be discussed below, as they will be important for the biomimicry of corresponding region-specific neural organoids.

### Forebrain vascularization

The telencephalon, i.e., rostral forebrain, is vascularized by a combination of the PNVP (discussed prior) and the periventricular vascular plexus (PVP; also referred to as the subventricular plexus; Figure 2A). There are competing hypotheses on the mechanisms by which the PVP arises. One viewpoint suggests that the periventricular vessels arise as branches of the PNVP.<sup>28–31</sup> For example, as the invading capillaries of the PNVP reach the apical neuroepithelium within forebrain ventricles, they begin to branch

### Figure 1. Anatomy and development of CNS vasculature

(A) The leftmost diagram shows the major vessels of the human embryo at CS 13 in relation to the forebrain, midbrain (Mb), hindbrain, and spinal cord (neural tube morphology outlined in yellow). Substructures of the nervous system, including the budding cranial nerves (CNI–XII) and cervical spinal nerve nuclei (C1–7) are also shown. The paired dorsal aortas, which run along the rostral-caudal axis of the embryo, give rise to the aortic arches and their derivatives, including the primitive internal carotid artery (ICA) and its finer branches. The primary head vein is also evident at this developmental stage. In the middle diagram, major brain arteries, including the circle of Willis, are shown in a sagittal view of a human embryo at CS 20. Vessels corresponding to the circle of Willis and its branches are shaded in white and labeled in green. The far-right diagram shows the transition of circle of Willis anatomy from CS 20 to CS 21. While most of the circle of Willis is well developed at CS 20, the anterior communicating artery (AComM) forms by CS 21. Vessels corresponding to those shown in the middle diagram are shaded in white. Left and middle diagrams are adapted from Bertulli and Robert<sup>1</sup> and Raybaud.<sup>2</sup> Right diagram is adapted from Takakuwa et al.<sup>4</sup> ACA, anterior cerebral artery; ICA, internal carotid artery; Mb, midbrain; MCA, middle cerebral artery; PCA, posterior cerebral artery; PComM, posterior communicating artery.

(B) The PNVP begins to develop at CS 9–10. Blood islands surrounding the developing neural tube form through the fusion of CD34<sup>+</sup> hemangioblasts and subsequent differentiation into CD31<sup>+</sup> endothelial progenitors. Further fusion results in PNVP formation. The diagram was created with BioRender.

(C) Vascularization of the neural tube follows the directionality of neural tube closure, which begins at ~CS 10 at the midbrain/hindbrain boundary and proceeds rostrally and caudally from this closure point. A second putative neural tube closure initiation site is located in the rostral forebrain. PNVP vessels penetrate the neural tube between ~CS 14 and ~CS 23, based on variable literature reports. Vessel penetration proceeds in a ventral-to-dorsal direction and rostrally or caudally from respective neural tube closure sites. The top diagram created with BioRender. The bottom diagram was adapted from Wallingford et al.<sup>5</sup>

(D) A transverse section of the neural tube is shown with radial penetration of PNVP vessels toward the luminal surface (right side). A more detailed diagram (left side) shows the progression of penetrating vessels throughout early cortical plate development. The thickness of the neural tissue between the PNVP and the CSF increases over time, and neural progenitors present in the subventricular zone differentiate into neuronal subtypes that occupy deep and superficial cortical layers. Primitive vessels from the PNVP penetrate the glial limiting membrane, and extensions of the subarachnoid space, called the Virchow-Robin compartment, accompany the vessels along their path. Over the course of development, penetrating vessels also branch laterally and form connections with neighboring vessels. The right diagram was adapted from Raybaud.<sup>2</sup> Both diagrams were created with BioRender.

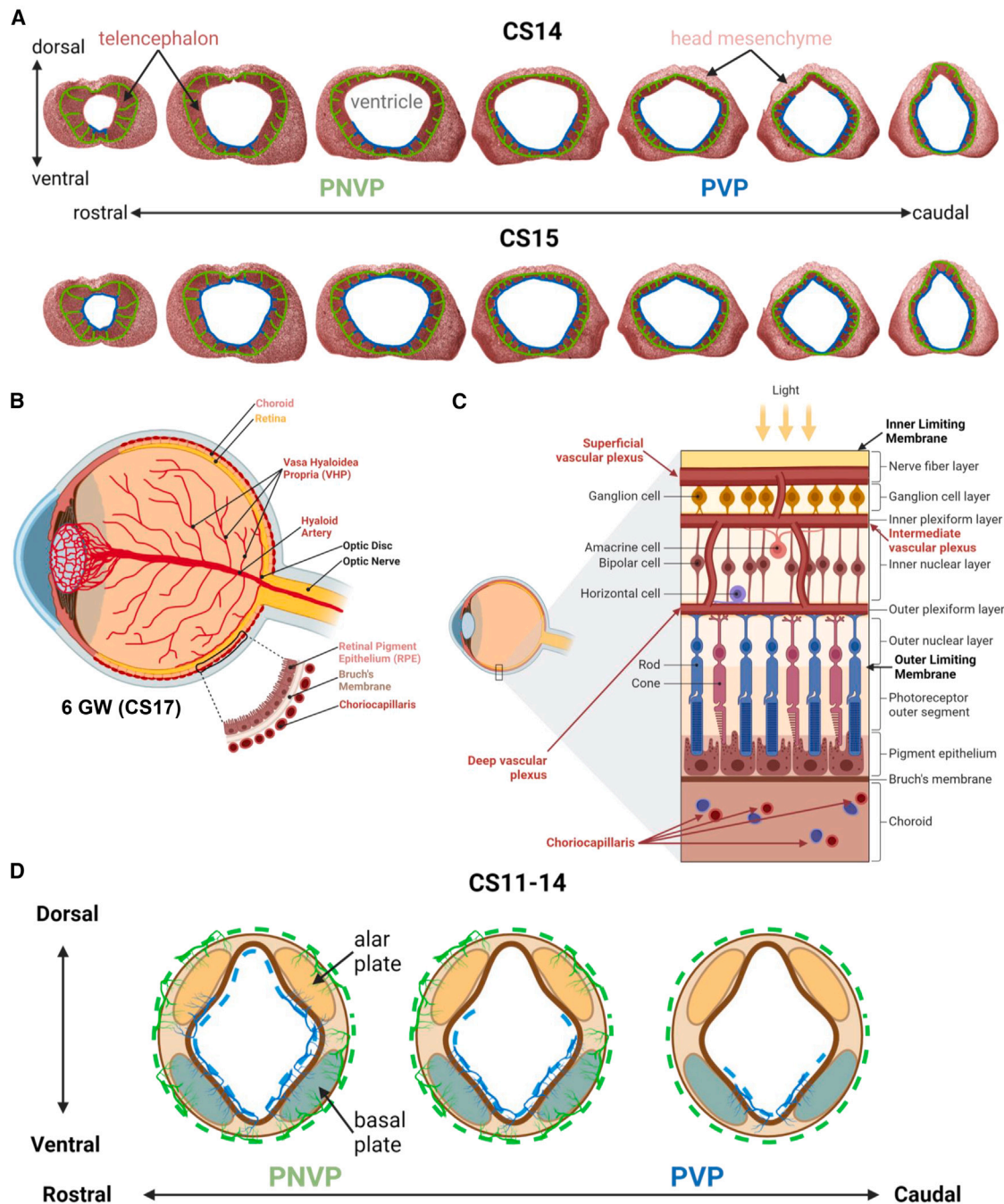


**Figure 2. Developmental vascular architecture of different CNS regions**

(A) Forebrain: between CS 14 and CS 15, the periventricular plexus (PVP; shown in blue near the ventricle), which is initially present in the ventral telencephalon, spreads to the dorsal telencephalon. Vascularization by the PVP also proceeds in a caudal to rostral direction. The perineural vascular plexus (PNVP; shown in green) is present before the establishment of the PVP and forms connections with the PVP. Telencephalic coronal plane slices were adapted from portions of Carnegie embryo sections from the Virtual Human Embryo resource (Endowment for Human Development, <https://www.ehd.org/virtual-human-embryo/>).

(B) Retina: before maturation of the retinal vasculature, two primary blood sources around the retina are the hyaloid artery and its branches (vasa hyaloidea propria), which supply blood to the developing lens and the surface of the inner retina, as well as the choriocapillaris, which supplies the retinal pigment epithelium and photoreceptors. The image was created with BioRender.

(C) The retinal vasculature is organized into three layers: the superficial, intermediate, and deep vascular plexuses, located in the GCL and NFL, IPL, and between the INL and OPL, respectively. The image was created with BioRender.

(legend continued on next page)

at right angles and anastomose to form the PVP in the subventricular zone (SVZ), a site of continual neurogenesis throughout development and adulthood. Another hypothesis is that PVP vasculature is derived from a basal vessel (originating from pharyngeal arch arteries) located deep on the floor of the telencephalic vesicle in the basal ganglia primordium<sup>3,15,22</sup> independent from the PNVP. In this scenario, by the time the PNVP superficially circumscribes the neural tube, a separate population of periventricular vessels is seen halfway between the pial and ventricular surfaces of the developing brain.<sup>15</sup> Yet, another hypothesis, and the most likely scenario, is that the PVP originates from a combination of branches of PNVP perforating vessels (PVs) as well as from the pharyngeal arch artery-derived basal vessel. Connection of the pial vessels of the PNVP and the periventricular vessels may represent the earliest form of arteriovenous communication in the telencephalon.<sup>15</sup> Based on the findings from 3D scanning electron microscope reconstructions of vascular corrosion casts of embryonic mouse brains, it is likely that the periventricular vessels develop into an arterial network and the pial vessels (from the PNVP) develop into venous sinuses.<sup>3</sup>

In mice, the PVP begins to form slightly after definitive establishment of the PNVP in the forebrain. In embryonic day (E)9 mice (CS 11), periventricular vessels are initially restricted to the ventral telencephalon,<sup>16</sup> and by E10 (CS 13/14), they have begun to form a plexus (PVP) in the ventral telencephalon<sup>15,16</sup> (Figure 2A). By E11 (CS 15), periventricular vessels are present in the dorsal telencephalon via migration from the ventral telencephalon. Migration of periventricular ECs also aligns with the migration path of GABA neurons during development. However, the ECs migrate in advance of the neurons.<sup>15,32</sup> Vascularization of the telencephalon by periventricular vessels is directed by EC-intrinsic expression of region-specific homeobox transcription factors that are typically associated with either ventral (*Nkx2.1*, *Dlx1/2*) or dorsal (*Pax6*) neural progenitors. These transcription factors are also responsible for the dorsal-ventral regionalization of the neuroepithelial tissue of the developing telencephalon.<sup>15</sup> The PVP extends not only in a ventral-to-dorsal direction but also in a medial-to-lateral direction, eventually extending across both lateral ventricles.<sup>15</sup> Furthermore, the ECs that comprise the PNVP and PVP vessels are transcriptionally distinct; genes associated with various processes in embryonic forebrain development including neurogenesis, differentiation, morphogenesis, migration, chemotaxis, and axon guidance are enriched in PVP ECs.<sup>32</sup>

### Retina vascularization

The timing of human versus rodent eye vascularization differs substantially. Human retinal vascular development begins during embryonic stages and is nearly complete at birth, whereas mouse retinal vasculature only starts to develop at birth and completes around 3 weeks postnatally.<sup>33–35</sup> Like the forebrain, two separate vascular systems are present at the start of embryonic eye development, but neither vascularizes the developing

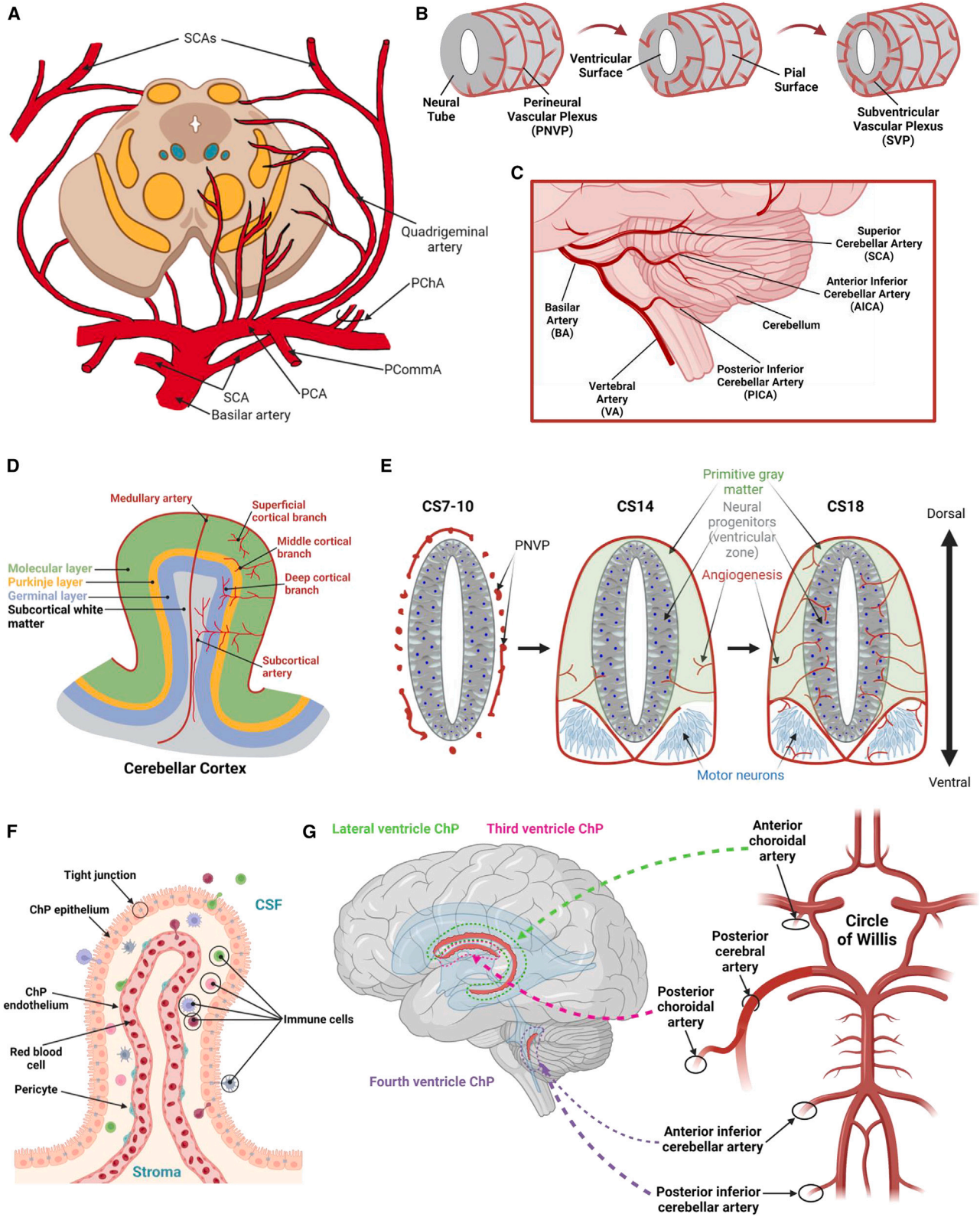
retina. The choriocapillaris supplies the outer surface of the developing retina, while the hyaloid arteries supply the inner surface of the developing retina and lens<sup>34</sup> (Figure 2B). Around the 4<sup>th</sup> GW (~CS 12), mesoderm near the optic cup differentiates into endothelium that will become the choriocapillaris, and the primitive dorsal ophthalmic artery branches to establish the hyaloid artery.<sup>36</sup> At 6 GWs (~CS 17), there is an extensive vascular network in the vitreous of the eye; however, patchy labeling for early endothelial markers in the choriocapillaris, including CD31, CD34, and CD39, indicates the immaturity of this structure. In the eyes of 6–8 GW human embryos (~CS 17–22), scattered CD39<sup>+</sup> retinal angioblasts are present in the inner retina but have not yet started to coalesce into a vascular plexus. Furthermore, there are no detectable pericytes (NG2<sup>+</sup>), smooth muscle cells (SMA<sup>+</sup>), or glial cells (Pax2<sup>+</sup>, GFAP<sup>+</sup>),<sup>37</sup> which are components of a mature blood-retina barrier (BRB). Eventually, the choriocapillaris and the hyaloid system anastomose to form a connection that acts as the hyaloid's venous drainage,<sup>36</sup> although the timing of this event is unclear.

Although the choriocapillaris persists into adulthood and ultimately envelops the entire exterior surface of the optic cup, the hyaloid vasculature begins to regress around the 2<sup>nd</sup> gestational month (~CS 22/23; Figure 2C). This occurs through macrophage-facilitated atrophy of hyaloid branches in the vitreous and lens capsule, terminating in atrophy of the hyaloid artery itself by the 3<sup>rd</sup> gestational month.<sup>34,36</sup> Additionally, while the choriocapillaris develops into a high-flow, fenestrated endothelium that allows for the exchange of gasses, nutrients, and metabolites, the vasculature of the inner retina forms a BRB that is homologous in function to the BBB, which characterizes most of the CNS vasculature.<sup>34</sup> An additional barrier is provided by the retinal pigment epithelium (RPE) tight junctions and the Bruch's membrane (i.e., the basement extracellular matrix [ECM] secreted by the RPE around the 6<sup>th</sup> GW), which separates the relatively leaky choriocapillaris from the neural retina.<sup>34</sup>

The appearance of the inner retinal vasculature in humans is significantly delayed relative to the initial development of the choriocapillaris and the hyaloid system.<sup>36</sup> Up to the 4<sup>th</sup> gestational month, the developing retina's metabolic needs are met by the branches of the hyaloid arteries.<sup>36</sup> By the 120 mm stage (~16 GWs), the mostly avascular retina consists of many of the layers present in the adult retina, including the RPE, outer and inner limiting membranes (OLMs and ILMs), outer and inner plexiform layers (OPLs and IPLs), inner nuclear layer (INL), ganglion cell layer (GCL), and nerve fiber layer (NFL); by mid-gestation, all layers of the adult retina are recognizable<sup>38</sup> (Figure 2C).

Vascularization of the human retina initiates through the process of vasculogenesis. Prior to 14–15 GWs, large numbers of spindle-shaped precursor cells migrate from the optic disk. By 14 GWs, blood vessels extend in two arcades (superior and inferior) just past the outer boundary of the optic nerve head.<sup>37</sup> At 14–15 GWs, the spindle-shaped cells, i.e., endothelial precursors, begin to align into an immature vascular tree in the inner

(D) Midbrain: the embryonic midbrain is vascularized between ~CS 10/11 and ~CS 14. Midbrain alar and basal plates are shown in yellow and teal, respectively. At this stage, the PNVP (shown in green) is present in all areas of the midbrain along the rostral-caudal axis, with penetrating vessels' abundance increased in rostral versus caudal regions. The PVP (shown in blue) and its associated penetrating vessels progress in rostral-to-caudal and ventral-to-dorsal orientations as well. The images were created with BioRender.



(legend on next page)

retinal layers<sup>39</sup> (Figure 2C). While earlier studies suggested that these spindle-shaped cells are mesenchymal in origin,<sup>39</sup> others have shown more recently that they may be VEGF-secreting GFAP<sup>+</sup> astrocytes.<sup>35</sup> Throughout the process of vessel formation, CD39<sup>+</sup> angioblasts remain ahead of the advancing vascular front into avascular retinal regions.<sup>37</sup> Following formation of an immature retinal vascular plexus, blood vessel density is increased through angiogenesis from the optic disk.<sup>39</sup> By 16 GWs, the 4-lobe butterfly shape commonly recognized in adult retinal vasculature has begun to form, with superior and inferior arcades extending into the temporal and nasal retina.<sup>37</sup> From 17 to 21 GWs, the plexus is extended by angiogenesis, and this process continues even after birth.

### Midbrain vascularization

Although there is very limited information describing vascularization of the human embryonic mesencephalon (midbrain), we can extrapolate some general trends about human embryonic midbrain microvasculature from mouse studies.<sup>16</sup> At E8.5 (~CS 10), PVs originating from the PNVP are visible near the rostral alar midbrain, while no PVs are seen in the caudal midbrain (Figure 2D). By E9.5 (~CS 12), the portion of the PNVP that covers the midbrain seems complete but more “stretched out” compared to the earlier time point, possibly due to the expansion of the underlying brain regions. At this point, PVs contribute to the formation of the PVP (vasculature that will be associated with the eventual third ventricle), particularly in the pretectum and rostral midbrain. The PVP is most developed near the basal plate up to the alar-basal boundary. Overall, there are fewer PVs in the alar midbrain, and a clear PVP is absent in this region. In the caudal midbrain, the PNVP is present, but there are not yet PVs. At E10 (~CS 13/14), PVs, primarily concentrated near the basal plate, are present in the rostral midbrain, although they are still absent in the caudal midbrain.<sup>16</sup> At E11.5 (~CS 14/15), PVs are present throughout the rostral-caudal axis of the midbrain but appear more abundant in the alar midbrain.<sup>16</sup>

Most of what is known about midbrain blood vessels relates to the extrinsic vasculature, particularly large arteries that are

branches of the circle of Willis<sup>1</sup> (Figure 3A, right). The midbrain (or mesencephalon) is vascularized anteriorly by branches of the BA, laterally by the posterior choroidal artery (PChA) and quadrigeminal artery, which are branches of the posterior cerebral artery (PCA), and posteriorly by the quadrigeminal arteries and superior cerebellar arteries (SCAs). Studies in human embryos indicate that the vascular supply from the PChA develops around CS 15/16 (36/40 days post-conception [dpc]) at the time of posterior communicating artery (PCommA) branching.<sup>1</sup> Later in development (~CS 18–19), the BA branches continue to develop as the mesencephalon and fourth ventricle regions become distinct.<sup>1</sup> There is no distinct pattern of microvascularization in specific regions of the midbrain (e.g., substantia nigra, which is implicated in pathogenesis of Parkinson’s disease).

### Hindbrain (including cerebellum) vascularization

In all vertebrates, the BA is the major vascular supply of the hindbrain. In mouse embryos, hindbrain vascularization begins around E9.75 (~CS 13). Blood vessels invade the hindbrain sprouting from the PNVP and grow radially toward the ventricular zone<sup>42</sup> (Figure 3B). From E10, these radial vessels extend parallel to the ventricular hindbrain surface, turning at near right angles.<sup>42</sup> Further, around E10.5 (~CS 14), a subventricular vascular plexus (SVP) begins to form as neighboring sprouts start to meet and anastomose.<sup>42</sup> The final vascular structure of the hindbrain is comprised of the proximal, middle, and distal posterior circulation territories, including several branches supplying the cerebellum.<sup>43</sup>

Branches of the basilar artery (BA) and vertebral artery (VA) provide the main blood supply to the cerebellum (Figure 3C). The BA branches into two paired arteries, the SCA and anterior inferior cerebellar artery (AICA); the VA branches to form the posterior inferior cerebellar artery (PICA).<sup>43,44</sup> The SCA is divided into medial and lateral branches. The medial branch is responsible for vascularizing the superior vermis and the neighboring portions of the cerebellar hemisphere surface. The lateral branch vascularizes the most lateral portion of the superior surface of the cerebellar hemisphere.<sup>44</sup> The AICA arises from the caudal or middle third of the BA and usually reaches the anterior surface

### Figure 3. Developmental and adult vascular architecture of different CNS regions, continued

(A) Midbrain, continued: adult vascular structure of a cross-section of the rostral midbrain is shown. Alar or basal plate-derived structures are colored yellow or teal, respectively. The image was adapted from Mihailoff et al.<sup>40</sup>

(B) Hindbrain: during development, vessels from the perineural vascular plexus (PNVP) ingress into the neural tissue and grow radially toward the hindbrain ventricular surface. During extension, the vessels turn at near right angles and anastomose, forming a subventricular vascular plexus (SVP).

(C) In the cerebellum, blood supply is provided by branches of the basilar and vertebral arteries (BAs and VAs, respectively). The BA branches into two paired arteries, the superior cerebellar artery (SCA) and anterior inferior cerebellar artery (AICA). The vertebral artery branches to form the posterior inferior cerebellar artery (PICA).

(D) Schematic of microvasculature of the cerebellar cortex and subcortical white matter, focusing on a single gyrus. The figure was adapted from Akima et al.<sup>41</sup>

(E) Spinal cord: between ~CS 7 and ~CS 10, the PNVP has begun to form around the embryonic spinal cord via fusion of blood islands. At ~CS 14, a complete PNVP is seen surrounding the spinal cord, with angiogenic penetrating vessels entering the ventricular zone from the ventral aspect of the cord but avoiding the motor neuron columns. Vessel penetration into the developing spinal cord proceeds in a ventral-to-dorsal orientation, and by ~CS 18, vessels derived from the PNVP are also observed in the MN columns.

(F) Choroid plexus (ChP): the ChP villous structure containing vasculature is shown. The choroid epithelium acts as an interface between the CSF and the choroid vasculature (blood-CSF barrier). The fenestrated choroid vasculature lacks tight junctions characteristic of a BBB. Immune cells are shown interacting with both ChP epithelium and endothelium.

(G) Schematic of the lateral, third, and fourth ventricles in the adult human brain, along with the main arterial branches of the circle of Willis, which supply the ChPs associated with each ventricle. Dotted arrows from the arteries to the brain are colored according to targeted plexus, and the relative contributions of specific arteries are indicated by dotted line weight.

The images were created at least partially with BioRender.

of the simple, superior, and inferior semilunar lobules, as well as the flocculus, the ChPs of the lateral ventricular recess, and the middle cerebellar peduncles.<sup>44</sup> The PICA is also divided into medial and lateral branches, which supply the inferior cerebellar vermis, the ChP of the fourth ventricle, and the inferior and posterior surfaces of the cerebellar hemispheres, respectively.<sup>44</sup> Venous drainage occurs through the cerebellar veins, divided into superior, inferior, and anterior cerebellar veins.<sup>44</sup>

The cerebellar cortex's microvasculature is comprised of cortical arteries, which consist of superficial, middle, and deep cortical branches, subcortical arteries, and medullary arteries<sup>41</sup> (Figure 3D). Although information about microvascularization of the cerebellar cortex during human neural development is lacking, these arteries likely originate from the PNVP on the surface of the cerebellar cortex and penetrate at right angles relative to the cerebellar gyri. The cortical artery branches terminate in molecular, Purkinje, and granular layers, respectively. The subcortical and medullary arteries terminate in the subcortical white matter.

### Spinal cord vascularization

In the posterior CNS, the PNVP remodels directly from the VA and the dorsal longitudinal anastomotic vessel, both of which originate from the posterior wall of the dorsal aorta.<sup>11</sup> Spinal PNVP formation starts around E8.5–E9.5 in mouse embryos (~CS 11/12) and around E3 in avian embryos<sup>45,46</sup> (Figure 3E). At around E10.5 in mouse embryos (~CS 14), the sprouting of vessels, which radially invade the primitive spinal cord, is initiated by the action of VEGF and Wnt7a/b expressed by the neural tissue.<sup>18,47,48</sup> Notably, the spinal cord lacks a PVP, unlike the forebrain and midbrain.<sup>45</sup>

Analogous to the forebrain, PNVP sprouting vessels first invade the ventral spinal cord adjacent to the floor plate (FP) and lateral to motor neuron (MN) columns<sup>22,45,49</sup> and proceed in the dorsal direction<sup>50</sup> (Figure 3E). By E10.5, these invading vessels continue growing dorsally but avoid the most dorsolateral regions, the MN clusters, the FP, and part of the neural progenitors' zone during this developmental time window. In mouse embryos, this regional avoidance continues through E12.5 (~CS 16).<sup>49</sup> This stereotyped vessel invasion and maintenance of avascular regions occurs despite the presence of high VEGF expression in the MN columns<sup>49</sup> and appears to be controlled via a cell intrinsic mechanism.<sup>50</sup> While MNs express VEGF to allow normal PNVP sprout invasion and vessel development, they also express sFlt1, a VEGF antagonist, to avoid premature vessel invasion into the MN columns.<sup>49</sup> Thus, stereotyped vascularization of the developing spinal cord is critical for the proper development of both neural and vascular structures and is regulated by both neuroepithelial progenitors and MNs via a VEGF/sFlt1 mechanism.

### ChP vascularization

The ChP is a highly vascularized secretory tissue responsible for producing cerebrospinal fluid (CSF) as well as regulating its composition.<sup>51</sup> The ChP consists of a vascular core, an interstitial stromal layer, and a monolayer of epithelial cells<sup>51</sup> (Figure 3F). There are also complex interactions between immune cells and the ChP epithelium and endothelium in health and disease,

which are discussed elsewhere.<sup>52–54</sup> Of the four ChPs in the CNS, the hindbrain ChP is the first to appear during development, beginning around E9.5 (~CS 12) and peaking between E11 and E12 in mouse embryo (~CS 14/15), followed by telencephalic ChP development.<sup>51,55,56</sup> Cell specification in the ChP occurs early in development—between E8.5 and E9.5 (~CS 11/12) in the murine brain—and involves close contact between ChP epithelial cells and vascular cells.<sup>51,57</sup> However, the development of ChP vasculature, including the tissue's exact developmental time course, is not completely understood.

In most vertebrates, there are four ChPs. They reside in each ventricle of the brain, i.e., two in each lateral telencephalon, one in the diencephalon, and a fourth in the hindbrain ventricle.<sup>51</sup> Arteries that branch from the circle of Willis supply blood to the ChPs (Figure 3G). The lateral ventricle ChPs (telencephalic) are supplied by the anterior choroidal arteries. The third ventricle ChP is supplied by the PChAs, arising from the PCA. The hindbrain ChP (in the fourth ventricle) is supplied by branches from the PICA and, to a lesser extent, by the AICA.<sup>58</sup> In humans, the PICAs and AICAs begin sprouting at ~CS 18 and ~CS 16–17, and the posterior artery terminates in the hindbrain ChP by ~CS 21–22.<sup>59</sup>

A recent study developed a single-cell and spatial atlas of developing, adult, and aged mouse ChP demonstrating that arterial, venous, and capillary EC identities are established across adult ages and ventricles.<sup>60</sup> In the study, arteriovenous zonation of lateral ventricle ChPs was characterized, and it showed that the arteries develop obliquely across the veins running along the ventricular free margin of the tissue.<sup>60</sup> This mirrors the human scenario, in which the arterial supply develops from the caudal region of the ChP and extends rostrally along the attached margin, while the veins elongate and extend in the free margin of the rostral area of the ChP.<sup>61</sup> Vascular outgrowth and increases in surface area are induced by Shh produced by the ChP epithelium. This Shh signaling also regulates pericytes, which seem to have an important role in coordinating the development of the ChP vasculature and epithelium as well.<sup>62</sup>

### NVU formation and heterogeneity

A critical stage of vascularizing any CNS tissue is formation of the neurovascular unit (NVU). The NVU is composed of BBB-forming vascular ECs, neural progenitors, neuronal and glial cells, perivascular mural cells, and the basement membrane (reviewed in-depth elsewhere<sup>63–68</sup>). The induction of BBB properties in brain microvascular ECs (BMECs) is a gradual process that begins as early as E10.5 (~CS 14) in mouse embryogenesis.<sup>18,63</sup> BMECs express increased or brain-selective marker expression,<sup>69,70</sup> including tight junction proteins claudin-5, occludin, LSR, and MARVELD2 that seal connections between individual ECs and restrict paracellular transport. Also, they express active nutrient and drug efflux transporters such as GLUT-1 and P-glycoprotein, which help maintain BBB homeostasis by regulating the uptake of nutrients and the removal of harmful compounds, respectively. Additionally, transcytosis in BMECs is greatly reduced compared to peripheral ECs due to the decreased expression of structural proteins caveolin-1 and PLVAP and increased expression of lipid flippase MFSD2A.<sup>71</sup>

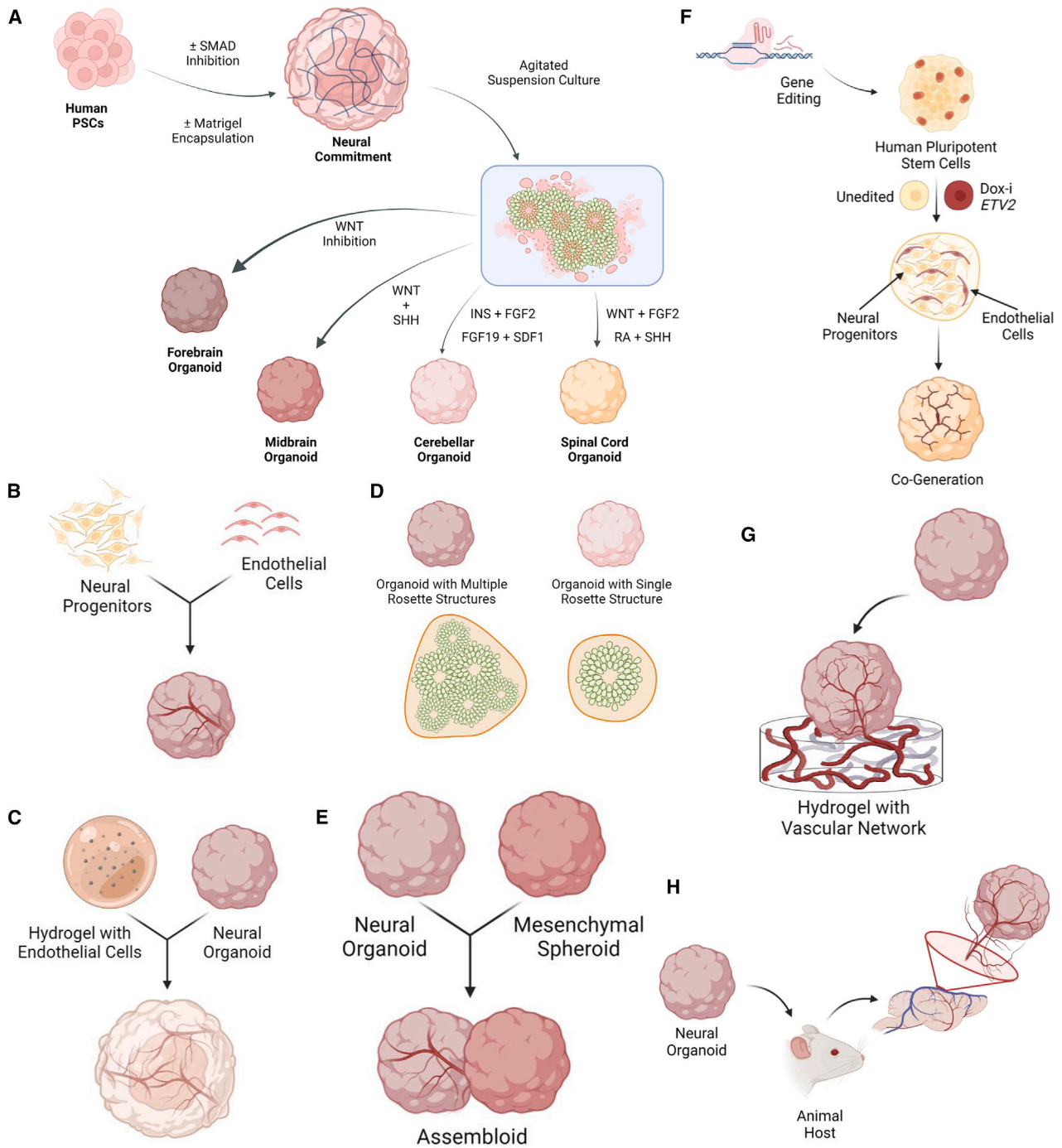


**Figure 4. Current methods for vascularizing neural organoids**

(A) Protocols for generation of generic and region-specific neural organoids. To generate 3D neural organoids, hPSC aggregates are cultured with or without (w/wo) Matrigel encapsulation or in the presence of small-molecule SMAD signaling inhibitors, which induces neural commitment. The organoids are typically cultured in agitated suspension culture, and the resulting structures contain numerous ventricular-like zones, a.k.a., neural rosettes. Incorporating combinations of Wnt activation or inhibition, Shh, FGF, RA, insulin, or chemokine receptor (SDF-1) signaling enables derivation of organoids corresponding to different brain regions (e.g., forebrain, midbrain, hindbrain, and spinal cord).

(B) Co-culture of hPSC-derived NPCs and ECs (either hPSC derived or primary) in a 3D format can produce neural organoids with a primitive endothelial network.

(C) ECs suspended within a hydrogel can invade an encapsulated neural organoid and self-assemble into a vascular network.

(D) Neural organoids derived from hPSCs typically exhibit multiple rosette structures. It is less common to find a neural organoid that contains a single rosette.

(legend continued on next page)

Although these markers distinguish BMECs, their expression varies by maturity. For example, claudin-5 and occludin staining is diffuse and cytoplasmic prior to 14 GWs.<sup>72</sup> Hence, endothelial BBB properties mature over time, as significant gene expression changes are observed in BMECs across mouse embryo development<sup>73</sup> and even between those in early postnatal versus adult mice.<sup>74</sup> Yet, the development of such mature BBB properties, which is a result of interactions between all NVU cell types, remains a challenge to recapitulate in neural organoids derived solely from hPSCs.

Recent single-cell RNA sequencing (scRNA-seq) atlases have characterized human brain vasculature, demonstrating that NVU cell types and structure display molecular and functional heterogeneity across development and aging.<sup>75–77</sup> For example, at 15 GWs, the occludin transcript is primarily expressed by tip ECs, but by 23 GWs, it is also expressed by arterial and mitotic ECs, with minimal expression in capillary or venous ECs.<sup>75</sup> Despite the early presence of BBB-like characteristics, there are fewer perfusable vessels at 17 versus 23 GWs, and the proportion of pericytes increases from 15 to 23 GWs.<sup>75</sup> Even after birth, mouse models of normal aging show that BMECs shift their transport profile from favoring specific receptor-mediated transcytosis to higher levels of nonspecific, caveolae-mediated trafficking of serum proteins.<sup>76</sup> This shift is coincident with decreased pericyte coverage of the brain microvasculature<sup>76</sup> and thus could also be posited to increase leakiness.<sup>19,78</sup>

Moreover, studies have provided insight into NVU differences between different CNS regions. For example, bulk and scRNA-seq have shown differences in ECs from the circumventricular organs, ChP, and choriocapillaris, where leakier vasculature is observed.<sup>79,80</sup> Tip ECs are highly enriched in the ventricular zone during human development, supporting the coincidence of angiogenesis and neurogenesis.<sup>75</sup> Also, compared to the pre-frontal and mid-temporal cortex, the hippocampus is characterized by a reduced abundance of ECs and pericytes and increased numbers of perivascular fibroblasts.<sup>81</sup> Additionally, not all CNS ECs exhibit the same level of BBB properties as those found in the cerebral cortex microvasculature. Reduced pericyte coverage and lower tight junction protein expression characterizes blood-spinal cord barriers.<sup>82</sup> Also, BBB properties are enhanced in white matter brain vessels compared to those in the gray matter vessels, correlating with higher vessel coverage by astrocyte endfeet in the white matter.<sup>83</sup> Whether such EC differences are cell intrinsic or extrinsic remains an open question.

RNA-seq studies have also revealed variability of brain ECs along the arteriovenous tree.<sup>84</sup> Postnatal and adult mouse brain and retina scRNA-seq studies identified markers differentiating venous, capillary, arterial, and pro-angiogenic tip EC phenotypes.<sup>69,84–86</sup> The distinct transcriptional profiles of these EC

subtypes has also been confirmed by human embryonic and adult scRNA-seq studies.<sup>75,81,87–89</sup> Further, the transcriptional variation across a variety of non-endothelial perivascular cells has also been characterized, including pericytes, smooth muscle cells, three types of perivascular fibroblasts, and ependymal cells.<sup>81</sup> In addition to the standard immunocytochemical labels, such NVU transcriptional profiles could also be used to assess the biomimicry of vascularized neural organoid models.

## BIOENGINEERING STRATEGIES FOR NEURAL ORGANOID VASCULARIZATION

In recent years, protocols have been developed to generate region-specific, human pluripotent stem cell (hPSC)-derived neural organoids (Figure 4A) corresponding to the dorsal<sup>90,91</sup> and ventral<sup>92–94</sup> forebrain, dorsomedial telencephalon (i.e., hippocampus and ChP),<sup>95</sup> diencephalon (e.g., thalamus, hypothalamus),<sup>96–98</sup> retina,<sup>99,100</sup> midbrain,<sup>101</sup> hindbrain (i.e., cerebellum and brainstem),<sup>102,103</sup> ChP,<sup>104</sup> and spinal cord.<sup>105</sup> However, most neural organoid protocols generate 3D tissues devoid of vasculature. Non-vascularized neural organoids are able to recapitulate an *in-vivo*-like diversity of regional neuronal and even glial cell types,<sup>90,106</sup> but their implementation for modeling neurological physiology, e.g., EC and neural progenitor cell (NPC) crosstalk in the neurogenic niche, pathologies, and toxicology is limited by the absence of a perfusable CNS-like vasculature with NVU components and BBB properties.<sup>22,107</sup> Additionally, non-vascularized neural organoids have limited *in vitro* growth potential due to hypoxia-induced necrosis.<sup>108</sup> Several authors report the presence of a necrotic core in un-vascularized neural organoids with positive staining for hypoxia marker HIF-1 $\alpha$ .<sup>109,110</sup> Thus, most neural organoids do not exceed a few millimeters in diameter (<4 mm), which is not comparable to the human neocortex size.<sup>14,96,109–112</sup> Also, they begin to shrink after 6–7 months in culture due to the lack of sufficient oxygen and nutrient delivery.<sup>113</sup> This motivates continued efforts to develop approaches for bioengineering perfusable vascular networks within neural organoids.

To induce vascularization, non-neural cell types, e.g., endothelial progenitors or ECs, have been integrated into or co-derived within neural organoids using several different approaches.<sup>108,114</sup> These can be categorized as inducing neural organoid vascularization by (1) physical co-culture with ECs, (2) co-derivation with ECs, or (3) relying on angiogenesis from pre-formed vascular networks (Figures 4B, 4C, and 4E–4H). Here, we review these strategies and evaluate their level of *in vivo* mimicry based on the type of organoid being vascularized and the information presented in [vascularization during human neural tube morphogenesis](#) (Table S2). Protocols for obtaining

(E) Vascular-neural assembloids can be created by combining an avascular neural organoid and vascular organoid in a culture medium that supports both tissue types and permits their fusion. Vessels from the vascular organoid invade the neural organoid.

(F) Neural organoids with rudimentary vessels can be generated using hPSCs gene edited to enable doxycycline-inducible overexpression of *ETV2*. When exposed to extrinsic culture conditions which promote neural differentiation and doxycycline, the co-aggregated and unedited hPSCs give rise to neural phenotypes, and the edited hPSCs differentiate into ECs. The result is co-generation of a neural organoid with a primitive network of endothelial vessels.

(G) EC vascular beds formed within hydrogels can be used to vascularize co-cultured hPSC-derived neural organoids.

(H) Neural organoids derived from hPSCs *in vitro* can be transplanted into the brain of an animal host to induce vascularization of the organoid, resulting in a perfusable, host-derived vascular network. All diagrams were created with BioRender.

endothelial and other NVU cell types incorporated into these vascularized organoids are demonstrated in [Figures S1–S3](#).

### Neural organoid vascularization via EC co-culture

Several strategies have been devised to derive ECs from various human sources, including primary and hPSC derived.<sup>115</sup> Even without brain microvasculature characteristics, the sheer presence of ECs via co-culture seems to influence organoid maturation. For example, Shi et al. developed a method capable of generating vascularized cortical organoids by co-culturing hPSCs with human umbilical vein endothelial cells (HUVECs) ([Figure 4B](#)).<sup>116</sup> These authors achieved a 3D structure consisting of typical human cortical cell types containing a vascular network, which was sustained for over 200 days in culture. In this system, HUVECs formed well-defined vascular structures, and the organoids recapitulated several features of neocortical development, displaying defined cell layers and a functional neuronal network. Moreover, these organoids were implanted in the S1 mouse cortex, where they integrated into the host cortical tissue and anastomosed with the native vascular system. Thus, it is possible that these vascularized neural organoids may prove superior to un-vascularized neural organoids in recapitulating human CNS development *in vitro*, providing a new platform to model brain disorders and assist the development of novel therapeutic strategies.<sup>117</sup> However, the structure of the HUVEC-derived vascular network differed significantly from that observed within the developing forebrain (see [vascularization during human neural tube morphogenesis](#)). While the HUVECs do create an extensive vascular network throughout the organoids' developing intermediate zone and cortical plate, they still initiate network formation within the organoid's developing cortical parenchyma versus modeling the PNVP's angiogenesis that invades from above the developing cortical plate and proceeds to the forebrain SVZ ([Figure 1D](#)). This resulted in HUVEC plexus formation superficial to the VZ/SVZ, with a complete absence of a PVP network structure. How this affects the radial glial cells that populate the organoids' VZ/SVZ during long-term culture is unknown, but the absence of a PNVP and PVP limits coupling of vascular phenomena to the developing cortex's neurogenic zone, a well-known *in vivo* phenomenon.<sup>118</sup> Thus, issues related to anatomical differences between the vascular networks created in these organoids and those found in the developing forebrain remain unresolved.

More recently, the derivation of ECs from hPSCs and their application in the development of vascularized neural organoids has also been demonstrated.<sup>119</sup> Pham et al. embedded cerebral neural organoids at day 34 of differentiation within a Matrigel hydrogel containing hPSC-derived ECs ([Figure 4C](#)).<sup>109</sup> These organoids were grown *in vitro* for up to 5 weeks to induce vascularization and then transplanted into immunodeficient mice. Embedding organoids within Matrigel containing ECs resulted in robust vascularization, and CD31<sup>+</sup> vessels were found around VZ/SVZ-like structures, a.k.a. neural rosettes, within the center of the organoids after transplantation ([Figure 4D](#)). However, the long-term impact of the observed vascularized organoid structure on the development of neural cells was not investigated. For example, how does the vascular network influence the behavior of radial glial cells within rosette structures? Addition-

ally, the vasculature was not evaluated for BBB properties, the capacity to regulate blood flow, or functional coupling with other neural cells.

Despite the inclusion of blood vessels, the previously discussed neural organoids remain void of stromal NVU components, e.g., pericytes and microglia. These components are derived from the mesoderm, and interactions between epithelial and mesenchymal components in the neural niche are also known to play a fundamental role during tissue development.<sup>114</sup> Assembloids, i.e., structures generated by spatially arranging multiple singular organoid types,<sup>107</sup> may help address this issue ([Figure 4E](#)). For example, Wörsdörfer et al. developed a method to simultaneously generate mesodermal aggregates and neural spheroids and subsequently fuse them together.<sup>120,121</sup> The mesenchymal component promoted vascularization and neural development.<sup>120</sup> In fact, the vascular network expanded with tissue growth and was responsive to pro-angiogenic conditions like hypoxia. Furthermore, the mesenchymal component also delivered microglia-like cells that infiltrated the neural tissue. In a similar study, these "mixed-lineage" assembloids were also created by fusion of hPSC-derived neural spheroids, EC spheroids, and supporting human mesenchymal stromal cells.<sup>122</sup> These structures were constructed using different cell ratios, and the authors found that incorporating stromal cells promoted secretion of cytokines like VEGF. The tri-spheroids also presented elevated levels of TBR1 (a cortical layer marker), NKX2.1 (a ventral neural marker), and Notch1 gene expression when compared to standard neural spheroids, indicating that neural-vascular-stromal juxtacrine/cell-cell contact interactions promoted organoid patterning. Additionally, BBB-specific gene expression and tight junction proteins were also enhanced in the mixed-lineage assembloids. A separate assembloid model showed that cortical organoids with pericyte integration demonstrated increased astrocytic maturation and production of basement membrane components.<sup>123</sup> Moreover, this model supported SARS-CoV-2 entry and replication within its neural cells, as the pericytes facilitated viral replication and spreading to astrocytes, thereby causing inflammatory type I interferon transcriptional responses. Lastly, after 30 days of co-culture, an assembloid model of induced PSC (iPSC)-derived vascular and cerebral organoids<sup>124</sup> showed spontaneous emergence of non-endothelial NVU cell types, including pericytes and astrocytes. Moreover, the constituent vasculature demonstrated BBB properties including upregulation of GLUT-1, claudin-5, and ZO-1 in ECs and BBB-like transendothelial electrical resistance (TEER) but not vascular perfusion. Such neurovascular/mesodermal assembloids are the closest *in vitro* mimics of CNS vascularization by the PNVP.

### Co-derivation of neural organoids with ECs

Given that nascent blood vessels acquire BBB properties upon penetrating into the developing neural tube,<sup>18,125,126</sup> the co-differentiation of ECs within neural organoids has been explored as a vascularization strategy.<sup>127</sup> Ham et al. demonstrated that VEGF supplementation during cerebral organoid derivation can induce the co-differentiation of ECs without constraining neural commitment.<sup>127</sup> These organoids formed blood vessel-like structures that, with Wnt7a supplementation, matured into vessels

expressing BBB-associated markers, such as claudin-5.<sup>127</sup> Nevertheless, natural CNS vascularization involves steps of angiogenesis, invasion, and sprouting from the PNVP and PVP. In contrast, the approach reported by Ham et al. relies on exogenous growth factor stimulation, which may not accurately replicate *in vivo* processes. Also, inter- and intra-organoid variability in the vessels' spatial orientation could affect their functional roles and interactions with neural tissues.

Genetic activation of the embryonic-restricted ETS variant transcription factor 2 (ETV2) is another approach to reprogram a subset of cells into ECs within neural organoids.<sup>128</sup> ETV2 expression produces adaptable ECs, which are capable of forming perfusable vascular networks both *in vitro* and *in vivo*.<sup>128,129</sup> Thus, these ETV2-expressing cells are phenotypically, transcriptionally, and functionally consistent with *bona fide* ECs. Cakir et al. took advantage of this approach to control ETV2 expression in hPSCs using a doxycycline-inducible system (Figure 4F).<sup>110</sup> Co-aggregation of wild-type hPSCs with up to 20% ETV2-expressing cells produced cortical organoids with complex vascular-like networks with improved functional maturation and acquisition of ECs expressing tight junction and harboring efflux transporter activity. Moreover, upon implantation, ETV2-induced endothelium supported the formation of perfusable blood vessels. While these vascularized cortical organoids display *in-vivo*-like interactions between neural cells and ECs,<sup>130</sup> this approach again deviates from the *in vivo* scenario where the PNVP invades the avascular neural tube. Thus, the result of such approaches appears to be the formation of a randomly structured vascular network both on the exterior and intervening throughout the organoid.

### Neural organoid vascularization via angiogenesis from pre-formed vascular networks

Culture platforms that allow precise spatial patterns of cell aggregates can enable standardization of neural organoid cytoarchitecture, thereby facilitating high-throughput screening applications.<sup>131–133</sup> For example, Knight et al. first demonstrated that biophysical control of tissue morphology induces controlled neural organoid emergence, specifically reproducible formation of organoids with a single neural rosette/VZ structure<sup>134</sup> (Figure 4D). Yet, these microtissues were not vascularized. We posit that the integration of 3D vascular networks,<sup>135</sup> for example by using biocompatible sacrificial materials<sup>136</sup> to overlay such engineered organoids with a pre-formed PNVP-like vascular networks, would further enhance their biological relevance.

In fact, some authors have suggested that perfusion of a pre-formed rudimentary vascular network in a vascularized organoid can promote maturation due to shear- and pulsatile flow-induced signaling in ECs and surrounding mural cells.<sup>120</sup> Several strategies to improve perfusion of vascularized organoids have been proposed in which organoids are co-cultured in an optimized ECM with a pre-established external microvascular network in a microfluidic chip<sup>137</sup> (Figure 4G). Such microphysiological systems may allow further study of neurovascular interactions in multiple contexts, ranging from pathogenesis associated with neurodegenerative diseases, to accurate prediction of BBB permeability to pharmaceuticals.<sup>138</sup> Kaushik et al., for example, used hPSC-derived ECs, neural progenitors, and microglia, together with primary pericytes, to engineer an approximation

of a vascular plexus *in vitro*.<sup>139</sup> However, this construct only features CD31<sup>+</sup> ECs forming cord-like structures without clear tube-like networks, no demonstration of perfusion, and unclear wrapping of pericytes around endothelial vessels.

Demonstrating perfusion of networks within vascularized neural organoids *in vitro* remains an unmet challenge. This is primarily due to the agitated suspension culture typically required to generate neural organoids.<sup>14</sup> To demonstrate this perfusion, researchers have taken advantage of the host capacity to vascularize neural organoids after direct implantation into rodents<sup>140,141</sup> (Figure 4H). Cakir et al. even showed that a proportion of vessels in their cerebral organoids were perfusable with fluorescein isothiocyanate (FITC)-dextran. However, these vessels were mainly localized to the outer portion of the organoid.<sup>110</sup> To our knowledge, robust perfusion of vascularized organoids has not been achieved *in vitro* but has required *in vivo* transplantation into mice.<sup>109,110,120,141</sup>

There has been significant progress in bioengineering vascularized, non-neural organoid microphysiological systems. For example, Nzou et al. developed a 3D spheroid model containing primary human BMECs, pericytes, and astrocytes and hPSC-derived microglia, oligodendrocytes, and neurons and demonstrated its potential for modeling the effects of hypoxia and inflammation on BBB function.<sup>142</sup> Also, Blanchard et al. created a hPSC-based 3D microphysiological model that recapitulated NVU properties, including the ability to replicate Alzheimer's disease (AD)-associated amyloid deposition and unveil the role of pericytes in the pathological features of APOE-4-mediated amyloid angiopathy.<sup>143</sup> However, neither of these microphysiological platforms harnessed the unprecedented mimicry and complexity of neural organoids. Thus, when fully realized, bioengineered and anatomically mimetic vascularized neural organoids have enormous potential as a tool for investigating neurological disease etiology and pathology as well as for therapeutic discovery.

### MODELING DEVELOPMENT AND DISEASE USING VASCULARIZED NEURAL ORGANIDS

Traditionally, animal (primarily murine) models have been used to study aspects of both developmental and adult neurological diseases. However, due to significant disparities between mouse and human development anatomically, e.g., neural tube closure and corticogenesis dynamics, and genetically, e.g., human-specific non-coding DNA regulatory elements and chromosomal architecture, the creation and utilization of human models to study neurovascular contributions to human neurological physiology and pathology is warranted.<sup>144–146</sup> Many complex neurodevelopmental disorders, e.g., Down syndrome (DS) and fragile X syndrome (FXS), have key human-specific features that impede the replication of their pathophysiology in mice.<sup>144</sup> Furthermore, mouse models of human neurodegenerative disease suffer from inconsistencies with the human presentation. For example, AD mouse models do not display human-like levels of neuronal loss despite an accumulation of amyloid  $\beta$  (A $\beta$ ).<sup>147</sup> Given such discrepancies, hPSC-derived CNS organoids have been used to study both development<sup>75,90,106,116,148,149</sup> and neurological disorders.<sup>14,117,150–153</sup> Yet, most existing CNS organoid models used in such studies are not vascularized.

Vascularized brain organoids have demonstrated improved expression of key BBB-associated proteins, including tight junction components (e.g., claudin-5, occludin, ZO-1) and ABC/SLC transporters (e.g., GLUT-1, P-glycoprotein, BCRP), and reduced nonspecific permeability to molecular cargoes.<sup>110,119,122,124,127</sup> Thus, facets of CNS organoid morphogenesis and disease modeling can be improved by vascularization. For example, un-vascularized organoids are limited in their ability to model later stages of CNS neurodevelopment (>CS 14), in part because they lack interaction of apical neuroepithelial cells/radial glia with PVP vasculature. One study observed an increased number of CTIP2 and NeuN-positive neurons, progeny of radial glial cells, just by integrating human fetal endothelial and mural cells versus 3T3 fibroblasts into cortical organoids.<sup>75</sup> *In vivo*, perfusable vasculature enables CNS tissue expansion by providing oxygen throughout the parenchyma. If replicated *in vitro*, then this would enable continual neural organoid growth by sustaining interior neurogenic ventricular zones, thereby allowing increased corticogenesis and possibly even enhanced neuronal migration events that establish proper circuitry.<sup>22</sup> The sustained growth and maturation could even facilitate exploration of neural organoids as potential transplants for the repair of damaged CNS tissues.<sup>140,154</sup> Additionally, oligodendrogenesis *in vivo* is preceded by angiogenesis, and evidence supports the importance of oligodendrocyte-vasculature coupling for trophic support and proper physiology.<sup>155,156</sup> While un-vascularized organoids have shown evidence of oligodendrocyte progenitor cells (OPCs),<sup>92,116,157</sup> the presence of mature myelinating oligodendrocytes is rare.<sup>158–161</sup> This aspect of *in vivo* CNS tissues is requisite for proper neuronal maturation to model circuit behavior and demyelinating diseases, e.g., multiple sclerosis, in which BBB crossing of immune cells is a significant component.<sup>162</sup> Lastly, vascularizing CNS organoids from a PNVP-like external vascular plexus could also provide insight into induction of BBB and BRB properties, including modeling barrier-crossing therapeutics. Dysfunction of these vascular barriers is a key feature in the pathogenesis of stroke<sup>163</sup>; AD,<sup>164</sup> Huntington's disease (HD),<sup>165</sup> and Parkinson's disease<sup>166</sup>; glioblastoma multiforme<sup>167</sup>; multiple sclerosis<sup>162,168</sup>; brain arteriovenous malformations (AVMs)<sup>169</sup>; retinopathy of prematurity<sup>170</sup>; and age-related macular degeneration.<sup>171</sup> Moreover, there is evidence of vascular involvement in the pathophysiology of neuropsychiatric diseases such as depression and schizophrenia,<sup>172</sup> highlighting that even diseases not previously recognized as neurovascular in nature may benefit from vascularized CNS organoids.

Stroke is a common cerebrovascular pathology for which perfusion is a key component of disease modeling and remains under-studied using CNS organoids. Although stroke is much more common in adults, there are also ischemic and hemorrhagic stroke-associated pathologies in neonates and children, which could be better studied using hPSC-derived CNS organoids. These include germinal matrix hemorrhage, which primarily affects premature neonates born before 32 GWs,<sup>173</sup> large vessel vasculopathies like steno-occlusive or Moyamoya diseases, which can occur secondary to sickle cell disease in children,<sup>174</sup> and AVMs, a leading cause of hemorrhagic stroke in the young.<sup>89</sup>

As a major strength of their potential clinical application, hPSC-derived vascularized CNS organoids provide an unprecedented

opportunity to investigate the genetic basis of CNS vascular diseases through the use of patient-derived iPSCs.<sup>152,175</sup> Furthermore, gene-edited hPSCs could be modified with targeted risk mutations or utilized in CRISPR-screening approaches.<sup>176</sup> This would enable the study of how genetic modifications in NVU cells affect the development and progression of CNS vascular diseases. Numerous monogenic and polygenic neuropathologies have been identified to entail a component of vascular disruption, including familial cerebral cavernous malformations (CCMs), microcephaly, cerebral autosomal-dominant arteriopathy with subcortical infarcts and leukoencephalopathy (CADASIL), and GLUT-1 deficiency (De Vivo) syndrome.<sup>64</sup> Complex, polygenic diseases in which certain regions of the brain are predominantly affected, e.g., the hippocampus in AD,<sup>177,178</sup> would also benefit from using organoids with region-specific vascularization to better understand disease pathogenesis and its genetic etiology. Some advancements have been made in this area, with a recent cerebral-vascular assembloid model recapitulating certain aspects of *in vivo* CCMs.<sup>124</sup>

Although there has been some success with modeling of developmental neuropathologies, the fetal-like phenotype of many CNS (particularly cortical) organoids may limit our ability to generalize findings from models of neurodegenerative diseases.<sup>106,179</sup> Vascularization is postulated to improve the overall maturity of neural cell types in CNS organoids, thereby possibly leading to the ability to more faithfully model postnatal and adult-onset diseases. Several non-vascular strategies have also been proposed, including overexpression of progerin (truncated version of lamin A associated with Hutchinson-Gilford progeria syndrome) and reactive oxygen species (ROS)-induced DNA and mitochondrial damage.<sup>180</sup> However, these methods do not address the reduced neuron number, maturation, or overall neural tissue cytoarchitecture that emerges *in vivo* via vascularization.

As an additional level of modeling complexity, scRNA-seq studies have uncovered cellular and molecular perturbations to the NVU due to various CNS pathologies.<sup>77,87–89</sup> Alterations in BBB properties also occur in the context of various CNS diseases, including AD<sup>87</sup> and HD<sup>88</sup> and brain AVMs.<sup>89</sup> For example many genes are downregulated in AD, with the greatest AD-related changes occurring in mural cells.<sup>87</sup> Also, the highest proportion of AD-related risk genes are upregulated in immune cells.<sup>87</sup> In HD, several BMEC genes related to nutrient and efflux transport and several mural cell genes with known HD-related mutations are downregulated.<sup>88</sup> For the case of patients with AVMs, ECs are relatively enriched for arterial and venous subtypes, with significantly fewer venular and capillary ECs compared to healthy controls.<sup>89</sup> Furthermore, ECs in patients with AVMs displayed decreased expression of nutrient transporters such as *SLC38A5* and *SLC16A1* as well as *MFSD2A*.<sup>89</sup> Thus, vascularized organoid modeling of CNS pathologies can benefit from the inherent multicellularity, but whether they can recapitulate some of the key changes observed in humans remains to be seen.

## CLOSING REMARKS AND FUTURE PERSPECTIVES

Modeling CNS development and disease using neural organoids would be significantly improved by the advent of physiologically

accurate CNS organoid vascularization protocols. The presence of ECs in the CNS has been shown to be important for neuronal maturation, and vascularized brain organoids possess a higher concentration of active neurons capable of conducting action potentials.<sup>110,181</sup> Even in the adult brain, SVZ vasculature is well known to create a critical niche for neural stem cells.<sup>182</sup> In [bioengineering strategies for neural organoid vascularization](#), we reviewed the varied and unique aspects of CNS vascularization during the earliest stages of embryonic development and across different CNS tissues. This developmental period is particularly applicable for neural organoid bioengineering. Integration of such vascularization aspects would yield *in vitro* models that both expand and improve the utility of neural organoids for modeling human neurological disease pathogenesis and discovering novel therapeutic strategies.

In [modeling development and disease using vascularized neural organoids](#), we highlighted contemporary methodologies for bioengineering vascularized neural organoids, identifying both their strengths and shortcomings. In summary, better integration of tissue engineering strategies is needed to enable the reproducible emergence of biomimetic vascular network structure within neural organoids. Moreover, these strategies need to help simplify vascularized neural organoid derivation to make it accessible and scalable. As discussed previously, organoid vascularization can be achieved *in vitro*<sup>183</sup> or by transplantation into a mouse recipient with subsequent vascularization by host ECs. However, given the inherent self-organization capacity of neural organoids, limited attention was initially given to improving the structural/anatomical reproducibility of the organoid's cytoarchitecture. However, early work by Lancaster et al. shows that integration of biocompatible microfilaments can assist cerebral organoid formation.<sup>111</sup> Microfilament-engineered organoids displayed enhanced features, including improved neuroectoderm formation and cortical development. Moreover, micropatterned substrates can be used to induce the reproducible emergence of 3D neural rosette tissues<sup>134</sup> and neuroepithelial tubes.<sup>131,132</sup> Therefore, tissue engineering strategies may, in theory, be used to guide vascularized organoid morphogenesis and increase their complexity and standardization as well.<sup>184</sup> As detailed in [modeling development and disease using vascularized neural organoids](#), achieving this feat could have transformative impacts on neurological disease modeling and therapeutic discovery.

One promising solution to bioengineer the guided formation of vascular structures within organoids is the utilization of sacrificial molding techniques.<sup>185</sup> For example, McNulty et al. have used poly(vinyl alcohol)-calcium salt templates fabricated by micro-injection molding to generate internal geometries within hydrogels.<sup>186</sup> Another strategy to generate complex and functional vascular architectures in hydrogels is the use of stereolithographic production with potent photoabsorbers.<sup>187</sup> Moreover, in recent years, substantial work was done in the development of 3D-printing techniques capable of rapidly producing arrays of organ-specific tissues.<sup>188–190</sup> In particular, “organ building blocks” resulting from hPSC-derived organoids were assembled into 3D constructs, integrating perfusable vascular channels via 3D bioprinting.<sup>191</sup> Integrating such techniques into neural organoid culture is non-trivial, as it could

have unforeseen effects on organoid morphogenesis. However, the time for such exploration is now, and it is needed across the many region-specific neural organoid models given the varied vascularization structures encountered during early human CNS development.

#### ACKNOWLEDGMENTS

S.M.B.'s research training was supported by NIGMS T32GM140935 and NHGRI T32HG002760. Research for this manuscript was supported by National Institutes of Health (NIH, USA) grants NINDS R01NS107461 (S.P.P. and E.V.S.), NHLBI R33HL154254 (S.P.P.), NINDS RF1NS132441 (E.V.S. and S.P.P.), NIEHS R42ES033912 (R.S.A.), NICHD R21HD103111 (R.S.A.), NCATS UG3/UH3 TR003150 (R.S.A.), and NSF ERC #1648035 (R.S.A.); Fundação para a Ciência e a Tecnologia (FCT, Portugal) grant SFRH/BSAB/150269/2019 (T.G.F.); Universidade de Lisboa Institute for Bioengineering and Biosciences (iBB) projects UIDB/04565/2020 (T.G.F.) and UIDP/04565/2020 (T.G.F.); and Associate Laboratory Institute for Health and Bioeconomy (i4HB) project LA/P/0140/2020 (T.G.F.).

#### AUTHOR CONTRIBUTIONS

T.G.F. and R.S.A. conceived the manuscript concept. S.M.B., T.P.S., T.G.F., and R.S.A. wrote the manuscript. S.M.B., S.P.P., E.V.S., T.G.F., and R.S.A. contributed to manuscript editing. S.M.B., T.G.F., and R.S.A. produced and edited figures.

#### DECLARATION OF INTERESTS

R.S.A. is a co-owner of Neurosetta, LLC, which commercializes micropatterned neural rosette technology.

#### SUPPLEMENTAL INFORMATION

Supplemental information can be found online at <https://doi.org/10.1016/j.celrep.2024.115068>.

#### REFERENCES

- Bertulli, L., and Robert, T. (2021). Embryological development of the human cranio-facial arterial system: a pictorial review. *Surg. Radiol. Anat.* 43, 961–973. <https://doi.org/10.1007/s00276-021-02684-y>.
- Raybaud, C. (2010). Normal and Abnormal Embryology and Development of the Intracranial Vascular System. *Neurosurg. Clin. N. Am.* 21, 399–426. <https://doi.org/10.1016/j.nec.2010.03.011>.
- Hiruma, T., Nakajima, Y., and Nakamura, H. (2002). Development of pharyngeal arch arteries in early mouse embryo. *J. Anat.* 201, 15–29. <https://doi.org/10.1046/j.1469-7580.2002.00071.x>.
- Takakuwa, T., Koike, T., Muranaka, T., Uwabe, C., and Yamada, S. (2016). Formation of the circle of Willis during human embryonic development. *Congenit. Anom. (Kyoto)* 56, 233–236. <https://doi.org/10.1111/cga.12165>.
- Wallingford, J.B., Niswander, L.A., Shaw, G.M., and Finnell, R.H. (2013). The continuing challenge of understanding, preventing, and treating neural tube defects. *Science* 339, 1222002. <https://doi.org/10.1126/science.1222002>.
- Kuban, K.C., and Gilles, F.H. (1985). Human Telencephalic Angiogenesis. *Ann. Neurol.* 17, 539–548. <https://doi.org/10.1002/ana.410170603>.
- Kurz, H. (2009). Cell lineages and early patterns of embryonic CNS vascularization. *Cell Adh. Migr.* 3, 205–210. <https://doi.org/10.4161/cam.3.2.7855>.
- Marín-Padilla, M. (2012). The human brain intracerebral microvascular system: Development and structure. *Front. Neuroanat.* 6, 38. <https://doi.org/10.3389/fnana.2012.00038>.

9. Hogan, K.A., Ambler, C.A., Chapman, D.L., and Bautch, V.L. (2004). The neural tube patterns vessels developmentally using the VEGF signaling pathway. *Development* 131, 1503–1513. <https://doi.org/10.1242/dev.01039>.
10. Gama Sosa, M.A., De Gasperi, R., Perez, G.M., Hof, P.R., and Elder, G.A. (2021). Hemovasculogenic origin of blood vessels in the developing mouse brain. *J. Comp. Neurol.* 529, 340–366. <https://doi.org/10.1002/cne.24951>.
11. Walls, J.R., Coultas, L., Rossant, J., and Henkelman, R.M. (2008). Three-dimensional analysis of vascular development in the mouse embryo. *PLoS One* 3, e2853. <https://doi.org/10.1371/journal.pone.0002853>.
12. de Bakker, B.S., Driessen, S., Boukens, B.J.D., van den Hoff, M.J.B., and Oostra, R.J. (2017). Single-site neural tube closure in human embryos revisited. *Clin. Anat.* 30, 988–999. <https://doi.org/10.1002/ca.22977>.
13. Allsopp, G., and Gamble, H.J. (1979). Light and electron microscopic observations on the development of the blood vascular system of the human brain. *J. Anat.* 128, 461–477.
14. Lancaster, M.A., Renner, M., Martin, C.A., Wenzel, D., Bicknell, L.S., Hurler, M.E., Homfray, T., Penninger, J.M., Jackson, A.P., and Knoblich, J.A. (2013). Cerebral organoids model human brain development and microcephaly. *Nature* 501, 373–379. <https://doi.org/10.1038/nature12517>.
15. Vasudevan, A., Long, J.E., Crandall, J.E., Rubenstein, J.L.R., and Bhide, P.G. (2008). Compartment-specific transcription factors orchestrate angiogenesis gradients in the embryonic brain. *Nat. Neurosci.* 11, 429–439. <https://doi.org/10.1038/nn2074>.
16. Puelles, L., Martínez-Marin, R., Melgarejo-Otalora, P., Ayad, A., Valavanis, A., and Ferran, J.L. (2019). Patterned vascularization of embryonic mouse forebrain, and neuromeric topology of major human subarachnoidal arterial branches: A prosomeric mapping. *Front. Neuroanat.* 13, 59. <https://doi.org/10.3389/fnana.2019.00059>.
17. Fantin, A., Vieira, J.M., Gestri, G., Denti, L., Schwarz, Q., Prykhodzij, S., Peri, F., Wilson, S.W., and Ruhrberg, C. (2010). Tissue macrophages act as cellular chaperones for vascular anastomosis downstream of VEGF-mediated endothelial tip cell induction. *Blood* 116, 829–840. <https://doi.org/10.1182/blood-2009-12-257832>.
18. Daneman, R., Agalliu, D., Zhou, L., Kuhnert, F., Kuo, C.J., and Barres, B.A. (2009). Wnt/ $\beta$ -catenin signaling is required for CNS, but not non-CNS, angiogenesis. *Proc. Natl. Acad. Sci. USA* 106, 641–646. <https://doi.org/10.1073/pnas.0805165106>.
19. Daneman, R., Zhou, L., Kebede, A.A., and Barres, B.A. (2010). Pericytes are required for blood-brain barrier integrity during embryogenesis. *Nature* 468, 562–566. <https://doi.org/10.1038/nature09513>.
20. Ben-Zvi, A., Lacoste, B., Kur, E., Andreone, B.J., Maysar, Y., Yan, H., and Gu, C. (2014). Mfsd2a is critical for the formation and function of the blood-brain barrier. *Nature* 509, 507–511. <https://doi.org/10.1038/nature13324>.
21. Virgintino, D., Maiorano, E., Errede, M., Vimercati, A., Greco, P., Selvaggi, L., Roncali, L., and Bertossi, M. (1998). Astroglia-microvessel relationship in the developing human telencephalon. *Int. J. Dev. Biol.* 42, 1165–1168.
22. Paredes, I., Himmels, P., and Ruiz de Almodóvar, C. (2018). Neurovascular Communication during CNS Development. *Dev. Cell* 45, 10–32. <https://doi.org/10.1016/j.devcel.2018.01.023>.
23. Nedergaard, M. (2013). Garbage truck of the brain. *Science* 340, 1529–1530. <https://doi.org/10.1126/science.1240514>.
24. Etchevers, H.C., Vincent, C., Le Douarin, N.M., and Couly, G.F. (2001). The cephalic neural crest provides pericytes and smooth muscle cells to all blood vessels of the face and forebrain. *Development* 128, 1059–1068. <https://doi.org/10.1242/dev.128.7.1059>.
25. Yamanishi, E., Takahashi, M., Saga, Y., and Osumi, N. (2012). Penetration and differentiation of cephalic neural crest-derived cells in the developing mouse telencephalon. *Dev. Growth Differ.* 54, 785–800. <https://doi.org/10.1111/dgd.12007>.
26. Korn, J., Christ, B., and Kurz, H. (2002). Neuroectodermal origin of brain pericytes and vascular smooth muscle cells. *J. Comp. Neurol.* 442, 78–88. <https://doi.org/10.1002/cne.1423>.
27. Faal, T., Phan, D.T.T., Davtyan, H., Scarfone, V.M., Varady, E., Blurton-Jones, M., Hughes, C.C.W., and Inlay, M.A. (2019). Induction of Mesoderm and Neural Crest-Derived Pericytes from Human Pluripotent Stem Cells to Study Blood-Brain Barrier Interactions. *Stem Cell Rep.* 12, 451–460. <https://doi.org/10.1016/j.stemcr.2019.01.005>.
28. Bär, T. (1983). Patterns of vascularization in the developing cerebral cortex. *Ciba Found. Symp.* 100, 20–36. <https://doi.org/10.1002/9780470720813.ch3>.
29. Ruhrberg, C., and Bautch, V.L. (2013). Neurovascular development and links to disease. *Cell. Mol. Life Sci.* 70, 1675–1684. <https://doi.org/10.1007/s00018-013-1277-5>.
30. Ruhrberg, C., Gerhardt, H., Golding, M., Watson, R., Ioannidou, S., Fujisawa, H., Betsholtz, C., and Shima, D.T. (2002). Spatially restricted patterning cues provided by heparin-binding VEGF-A control blood vessel branching morphogenesis. *Genes Dev.* 16, 2684–2698. <https://doi.org/10.1101/gad.242002>.
31. Doetsch, F., Caillé, I., Lim, D.A., García-Verdugo, J.M., and Alvarez-Buylla, A. (1999). Subventricular Zone Astrocytes Are Neural Stem Cells in the Adult Mammalian Brain. *Cell* 97, 703–716. [https://doi.org/10.1016/s0092-8674\(00\)80783-7](https://doi.org/10.1016/s0092-8674(00)80783-7).
32. Won, C., Lin, Z., Kumar T, P., Li, S., Ding, L., Elkhali, A., Szabó, G., and Vasudevan, A. (2013). Autonomous vascular networks synchronize GABA neuron migration in the embryonic forebrain. *Nat. Commun.* 4, 2149. <https://doi.org/10.1038/ncomms3149>.
33. Luty, G.A., and McLeod, D.S. (2018). Development of the hyaloid, choroidal and retinal vasculatures in the fetal human eye. *Prog. Retin. Eye Res.* 62, 58–76. <https://doi.org/10.1016/j.preteyeres.2017.10.001>.
34. Tata, M., Ruhrberg, C., and Fantin, A. (2015). Vascularisation of the central nervous system. *Mech. Dev.* 138 Pt 1, 26–36. <https://doi.org/10.1016/j.mod.2015.07.001>.
35. Gariano, R.F. (2010). Special features of human retinal angiogenesis. *Eye* 24, 401–407. <https://doi.org/10.1038/eye.2009.324>.
36. Anand-Apte, B., and Hollyfield, J.G. (2010). Developmental anatomy of the retinal and choroidal vasculature. In *Encyclopedia of the Eye*, J. Be-sharse and D. Bok, eds. (Elsevier Books), pp. 9–15. <https://doi.org/10.1016/B978-0-12-374203-2.00169-X>.
37. McLeod, D.S., Hasegawa, T., Prow, T., Merges, C., and Luty, G. (2006). The initial fetal human retinal vasculature develops by vasculogenesis. *Dev. Dyn.* 235, 3336–3347. <https://doi.org/10.1002/dvdy.20988>.
38. O’Rahilly, R. (1975). The prenatal development of the human eye. *Exp. Eye Res.* 21, 93–112. [https://doi.org/10.1016/0014-4835\(75\)90075-5](https://doi.org/10.1016/0014-4835(75)90075-5).
39. Hughes, S., Yang, H., and Chan-Ling, T. (2000). Vascularization of the human fetal retina: Roles of vasculogenesis and angiogenesis. *Invest. Ophthalmol. Vis. Sci.* 41, 1217–1228.
40. Mihailoff, G.A., Haines, D.E., and May, P.J. (2018). The Midbrain. In *Fundamental Neuroscience for Basic and Clinical Applications*, Elsevier pp. 183–194.
41. Akima, M., Nonaka, H., Kagesawa, M., and Tanaka, K. (1987). A study on the microvasculature of the cerebellar cortex - The fundamental architecture and its senile change in the cerebellar hemisphere. *Acta Neuropathol.* 75, 69–76. <https://doi.org/10.1007/BF00686795>.
42. Fantin, A., Vieira, J.M., Plein, A., Maden, C.H., and Ruhrberg, C. (2013). The embryonic mouse hindbrain as a qualitative and quantitative model for studying the molecular and cellular mechanisms of angiogenesis. *Nat. Protoc.* 8, 418–429. <https://doi.org/10.1038/nprot.2013.015>.
43. Wang, Q., and Caplan, L.R. (2016). Essentials of cerebellum and cerebellar disorders: A primer for graduate students. In *Essentials of*

- Cerebellum and Cerebellar Disorders: A Primer for Graduate Students, (Springer) pp. 39–54. <https://doi.org/10.1007/978-3-319-24551-5>.
44. Naidich, T.P., Duvernoy, H.M., Delman, B.N., Gregory, S.A., Kollias, S.S., and Haacke, M.E. (2009). Vascularization of the Cerebellum and the Brain Stem. In Duvernoy's Atlas of the Human Brain Stem and Cerebellum, Springer pp. 159–217.
  45. Vieira, J.R., Shah, B., and Ruiz de Almodovar, C. (2020). Cellular and Molecular Mechanisms of Spinal Cord Vascularization. *Front. Physiol.* *11*, 599897. <https://doi.org/10.3389/fphys.2020.599897>.
  46. Kurz, H., Gärtner, T., Eggli, P.S., and Christ, B. (1996). First blood vessels in the avian neural tube are formed by a combination of dorsal angioblast immigration and ventral sprouting of endothelial cells. *Dev. Biol.* *173*, 133–147. <https://doi.org/10.1006/dbio.1996.0012>.
  47. Stenman, J.M., Rajagopal, J., Carroll, T.J., Ishibashi, M., McMahon, J., and McMahon, A.P. (2008). Canonical Wnt Signaling Regulates Organ-Specific Assembly and Differentiation of CNS Vasculature. *Science* *322*, 1247–1250. <https://doi.org/10.1126/science.1164594>.
  48. James, J.M., Gewolb, C., and Bautch, V.L. (2009). Neurovascular development uses VEGF-A signaling to regulate blood vessel ingression into the neural tube. *Development* *136*, 833–841. <https://doi.org/10.1242/dev.028845>.
  49. Himmels, P., Paredes, I., Adler, H., Karakatsani, A., Luck, R., Marti, H.H., Ermakova, O., Rempel, E., Stoeckli, E.T., and Ruiz De Almodóvar, C. (2017). Motor neurons control blood vessel patterning in the developing spinal cord. *Nat. Commun.* *8*, 14583. <https://doi.org/10.1038/ncomms14583>.
  50. Takahashi, T., Takase, Y., Yoshino, T., Saito, D., Tadokoro, R., and Takahashi, Y. (2015). Angiogenesis in the developing spinal cord: Blood vessel exclusion from neural progenitor region is mediated by VEGF and its antagonists. *PLoS One* *10*, e0116119. <https://doi.org/10.1371/journal.pone.0116119>.
  51. Lun, M.P., Monuki, E.S., and Lehtinen, M.K. (2015). Development and functions of the choroid plexus-cerebrospinal fluid system. *Nat. Rev. Neurosci.* *16*, 445–457. <https://doi.org/10.1038/nrn3921>.
  52. Meeker, R.B., Williams, K., Killebrew, D.A., and Hudson, L.C. (2012). Cell trafficking through the choroid plexus. *Cell Adh. Migr.* *6*, 390–396. <https://doi.org/10.4161/cam.21054>.
  53. Schwerk, C., Tenenbaum, T., Kim, K.S., and Schrotten, H. (2015). The choroid plexus—a multi-role player during infectious diseases of the CNS. *Front. Cell. Neurosci.* *9*, 80. <https://doi.org/10.3389/fncel.2015.00080>.
  54. Figueiredo, C.A., Steffen, J., Morton, L., Arumugam, S., Liesenfeld, O., Deli, M.A., Kröger, A., Schüller, T., and Dunay, I.R. (2022). Immune response and pathogen invasion at the choroid plexus in the onset of cerebral toxoplasmosis. *J. Neuroinflammation* *19*, 17. <https://doi.org/10.1186/s12974-021-02370-1>.
  55. Currie, D.S., Cheng, X., Hsu, C.M., and Monuki, E.S. (2005). Direct and indirect roles of CNS dorsal midline cells in choroid plexus epithelia formation. *Development* *132*, 3549–3559. <https://doi.org/10.1242/dev.01915>.
  56. Dziegielewska, K.M., Ek, J., Habgood, M.D., and Saunders, N.R. (2001). Development of the choroid plexus. *Microsc. Res. Tech.* *52*, 5–20. [https://doi.org/10.1002/1097-0029\(20010101\)52:1<5::AID-JEMT3>3.0.CO;2-J](https://doi.org/10.1002/1097-0029(20010101)52:1<5::AID-JEMT3>3.0.CO;2-J).
  57. Thomas, T., and Dziadek, M. (1993). Capacity to form choroid plexus-like cells in vitro is restricted to specific regions of the mouse neural ectoderm. *Development* *117*, 253–262. <https://doi.org/10.1242/dev.117.1.253>.
  58. Damkier, H., and Praetorius, J. (2020). Structure of the mammalian choroid plexus. In *Role of the Choroid Plexus in Health and Disease* (Springer), pp. 1–33.
  59. Macchi, V., Porzionato, A., Guidolin, D., Parenti, A., and De Caro, R. (2005). Morphogenesis of the posterior inferior cerebellar artery with three-dimensional reconstruction of the late embryonic verteobasilar system. *Surg. Radiol. Anat.* *27*, 56–60. <https://doi.org/10.1007/s00276-004-0303-6>.
  60. Dani, N., Herbst, R.H., McCabe, C., Green, G.S., Kaiser, K., Head, J.P., Cui, J., Shipley, F.B., Jang, A., Dionne, D., et al. (2021). A cellular and spatial map of the choroid plexus across brain ventricles and ages. *Cell* *184*, 3056–3074.e21. <https://doi.org/10.1016/j.cell.2021.04.003>.
  61. Hudson, A.J. (1960). The development of the vascular pattern of the choroid plexus of the lateral ventricles. *J. Comp. Neurol.* *115*, 171–186. <https://doi.org/10.1002/cne.901150206>.
  62. Nielsen, C.M., and Dymecki, S.M. (2010). Sonic hedgehog is required for vascular outgrowth in the hindbrain choroid plexus. *Dev. Biol.* *340*, 430–437. <https://doi.org/10.1016/j.ydbio.2010.01.032>.
  63. Obermeier, B., Daneman, R., and Ransohoff, R.M. (2013). Development, maintenance and disruption of the blood-brain barrier. *Nat. Med.* *19*, 1584–1596. <https://doi.org/10.1038/nm.3407>.
  64. Zhao, Z., Nelson, A.R., Betsholtz, C., and Zlokovic, B.V. (2015). Establishment and Dysfunction of the Blood-Brain Barrier. *Cell* *163*, 1064–1078. <https://doi.org/10.1016/j.cell.2015.10.067>.
  65. Winkler, E.A., Bell, R.D., and Zlokovic, B.V. (2011). Central nervous system pericytes in health and disease. *Nat. Neurosci.* *14*, 1398–1405. <https://doi.org/10.1038/nn.2946>.
  66. Schaeffer, S., and Iadecola, C. (2021). Revisiting the neurovascular unit. *Nat. Neurosci.* *24*, 1198–1209. <https://doi.org/10.1038/s41593-021-00904-7>.
  67. McConnell, H.L., and Mishra, A. (2022). Cells of the Blood-Brain Barrier: An Overview of the Neurovascular Unit in Health and Disease. In *The Blood-Brain Barrier Methods and Protocols*, N. Stone, ed. (Springer Nature), pp. 3–24. <https://doi.org/10.1007/978-1-0716-2289-6>.
  68. Du, F., Shusta, E.V., and Palecek, S.P. (2023). Extracellular matrix proteins in construction and function of in vitro blood-brain barrier models. *Front. Chem. Eng.* *5*, 1130127. <https://doi.org/10.3389/fceng.2023.1130127>.
  69. Sabbagh, M.F., Heng, J.S., Luo, C., Castanon, R.G., Nery, J.R., Rattner, A., Goff, L.A., Ecker, J.R., and Nathans, J. (2018). Transcriptional and epigenomic landscapes of CNS and non-CNS vascular endothelial cells. *Elife* *7*, e36187. <https://doi.org/10.7554/eLife.36187>.
  70. Jambusaria, A., Hong, Z., Zhang, L., Srivastava, S., Jana, A., Toth, P.T., Dai, Y., Malik, A.B., and Rehman, J. (2020). Endothelial heterogeneity across distinct vascular beds during homeostasis and inflammation. *Elife* *9*, e51413. <https://doi.org/10.7554/eLife.51413>.
  71. Profaci, C.P., Munji, R.N., Pulido, R.S., and Daneman, R. (2020). The blood-brain barrier in health and disease: Important unanswered questions. *J. Exp. Med.* *217*, e20190062. <https://doi.org/10.1084/jem.20190062>.
  72. Virgintino, D., Errede, M., Robertson, D., Capobianco, C., Girolamo, F., Vimercati, A., Bertossi, M., and Roncali, L. (2004). Immunolocalization of tight junction proteins in the adult and developing human brain. *Histochem. Cell Biol.* *122*, 51–59. <https://doi.org/10.1007/s00418-004-0665-1>.
  73. Hupe, M., Li, M.X., Kneitz, S., Davydova, D., Yokota, C., Kele, J., Hot, B., Stenman, J.M., and Gessler, M. (2017). Gene expression profiles of brain endothelial cells during embryonic development at bulk and single-cell levels. *Sci. Signal.* *10*, eaag2476. <https://doi.org/10.1126/scisignal.aag2476>.
  74. Daneman, R., Zhou, L., Agalliu, D., Cahoy, J.D., Kaushal, A., and Barres, B.A. (2010). The mouse blood-brain barrier transcriptome: A new resource for understanding the development and function of brain endothelial cells. *PLoS One* *5*, e13741. <https://doi.org/10.1371/journal.pone.0013741>.
  75. Crouch, E.E., Bhaduri, A., Andrews, M.G., Cebrian-silla, A., Diafos, L.N., Birrueta, J.O., Wedderburn-Pugh, K., Valenzuela, E.J., Bennett, N.K., Eze, U.C., et al. (2022). Ensembles of endothelial and mural cells promote

- angiogenesis in prenatal human brain. *Cell* 185, 3753–3769.e18. <https://doi.org/10.1016/j.cell.2022.09.004>.
76. Yang, A.C., Stevens, M.Y., Chen, M.B., Lee, D.P., Stähli, D., Gate, D., Contrepolis, K., Chen, W., Iram, T., Zhang, L., et al. (2020). Physiological blood–brain transport is impaired with age by a shift in transcytosis. *Nature* 583, 425–430. <https://doi.org/10.1038/s41586-020-2453-z>.
  77. Wälchli, T., Ghobrial, M., Schwab, M., Takada, S., Zhong, H., Suntharalingham, S., Vetsiska, S., Gonzalez, D.R., Wu, R., Rehrauer, H., et al. (2024). Single-cell atlas of the human brain vasculature across development, adulthood and disease. *Nature* 632, 603–613. <https://doi.org/10.1038/s41586-024-07493-y>.
  78. Vazquez-Liebanas, E., Nahar, K., Bertuzzi, G., Keller, A., Betsholtz, C., and Mäe, M.A. (2022). Adult-induced genetic ablation distinguishes PDGFB roles in blood-brain barrier maintenance and development. *J. Cereb. Blood Flow Metab.* 42, 264–279. <https://doi.org/10.1177/0271678X211056395>.
  79. Wang, Y., Sabbagh, M.F., Gu, X., Rattner, A., Williams, J., and Nathans, J. (2019). Beta-catenin signaling regulates barrier-specific gene expression in circumventricular organ and ocular vasculatures. *Elife* 8, e43257. <https://doi.org/10.7554/eLife.43257>.
  80. Pfau, S.J., Langen, U.H., Fisher, T.M., Prakash, I., Nagpurwala, F., Lozoya, R.A., Lee, W.C.A., Wu, Z., and Gu, C. (2024). Characteristics of blood – brain barrier heterogeneity between brain regions revealed by profiling vascular and perivascular cells. *Nat. Neurosci.* 27, 1892–1903. <https://doi.org/10.1038/s41593-024-01743-y>.
  81. Sun, N., Akay, L.A., Murdock, M.H., Park, Y., Galiana-Melendez, F., Bubnys, A., Galani, K., Mathys, H., Jiang, X., Ng, A.P., et al. (2023). Single-nucleus multiregion transcriptomic analysis of brain vasculature in Alzheimer’s disease. *Nat. Neurosci.* 26, 970–982. <https://doi.org/10.1038/s41593-023-01334-3>.
  82. Wilhelm, I., Nyúl-Tóth, Á., Suciú, M., Hermenean, A., and Krizbai, I.A. (2016). Heterogeneity of the blood-brain barrier. *Tissue Barriers* 4, e1143544. <https://doi.org/10.1080/21688370.2016.1143544>.
  83. Nyúl-Tóth, Á., Suciú, M., Molnár, J., Fazakas, C., Haskó, J., Herman, H., Farkas, A.E., Kaszaki, J., Hermenean, A., Wilhelm, I., et al. (2016). Differences in the molecular structure of the blood-brain barrier in the cerebral cortex and white matter: An in silico, in vitro, and ex vivo study. *Am. J. Physiol. - Hear. Circ. Physiol.* 310, H1702–H1714. <https://doi.org/10.1152/ajpheart.00774.2015>.
  84. Vanlandewijck, M., He, L., Mäe, M.A., Andrae, J., Ando, K., Del Gaudio, F., Nahar, K., Lebouvier, T., Laviña, B., Gouveia, L., et al. (2018). A molecular atlas of cell types and zonation in the brain vasculature. *Nature* 554, 475–480. <https://doi.org/10.1038/nature25739>.
  85. Kalucka, J., de Rooij, L.P.M.H., Goveia, J., Rohlenova, K., Dumas, S.J., Meta, E., Conchinha, N.V., Taverna, F., Teuwen, L.A., Veys, K., et al. (2020). Single-Cell Transcriptome Atlas of Murine Endothelial Cells. *Cell* 180, 764–779.e20. <https://doi.org/10.1016/j.cell.2020.01.015>.
  86. Zarkada, G., Howard, J.P., Xiao, X., Park, H., Bizou, M., Leclerc, S., Künzel, S.E., Boisseau, B., Li, J., Cagnone, G., et al. (2021). Specialized endothelial tip cells guide neuroretina vascularization and blood-retina-barrier formation. *Dev. Cell* 56, 2237–2251.e6. <https://doi.org/10.1016/j.devcel.2021.06.021>.
  87. Yang, A.C., Vest, R.T., Kern, F., Lee, D.P., Agam, M., Maat, C.A., Losada, P.M., Chen, M.B., Schaum, N., Khoury, N., et al. (2022). A human brain vascular atlas reveals diverse mediators of Alzheimer’s risk. *Nature* 603, 885–892. <https://doi.org/10.1038/s41586-021-04369-3>.
  88. Garcia, F.J., Sun, N., Lee, H., Godlewski, B., Mathys, H., Galani, K., Zhou, B., Jiang, X., Ng, A.P., Mantero, J., et al. (2022). Single-cell dissection of the human brain vasculature. *Nature* 603, 893–899. <https://doi.org/10.1038/s41586-022-04521-7>.
  89. Winkler, E.A., Kim, C.N., Ross, J.M., Garcia, J.H., Gil, E., Oh, I., Chen, L.Q., Wu, D., Catapano, J.S., Raygor, K., et al. (2022). A single-cell atlas of the normal and malformed human brain vasculature. *Science* 375, eabi7377. <https://doi.org/10.1126/science.abi7377>.
  90. Velasco, S., Kedaigle, A.J., Simmons, S.K., Nash, A., Rocha, M., Quadrato, G., Paulsen, B., Nguyen, L., Adiconis, X., Regev, A., et al. (2019). Individual brain organoids reproducibly form cell diversity of the human cerebral cortex. *Nature* 570, 523–527. <https://doi.org/10.1038/s41586-019-1289-x>.
  91. Yoon, S.J., Elahi, L.S., Paşca, A.M., Marton, R.M., Gordon, A., Revah, O., Miura, Y., Walczak, E.M., Holdgate, G.M., Fan, H.C., et al. (2019). Reliability of human cortical organoid generation. *Nat. Methods* 16, 75–78. <https://doi.org/10.1038/s41592-018-0255-0>.
  92. Birey, F., Andersen, J., Makinson, C.D., Islam, S., Wei, W., Huber, N., Fan, H.C., Metzler, K.R.C., Panagiotakos, G., Thom, N., et al. (2017). Assembly of functionally integrated human forebrain spheroids. *Nature* 545, 54–59. <https://doi.org/10.1038/nature22330>.
  93. Bagley, J.A., Reumann, D., Bian, S., Lévi-Strauss, J., and Knoblich, J.A. (2017). Fused cerebral organoids model interactions between brain regions. *Nat. Methods* 14, 743–751. <https://doi.org/10.1038/nmeth.4304>.
  94. Xiang, Y., Tanaka, Y., Patterson, B., Kang, Y.J., Govindaiah, G., Rose-laar, N., Cakir, B., Kim, K.Y., Lombroso, A.P., Hwang, S.M., et al. (2017). Fusion of Regionally Specified hPSC-Derived Organoids Models Human Brain Development and Interneuron Migration. *Cell Stem Cell* 21, 383–398.e7. <https://doi.org/10.1016/j.stem.2017.07.007>.
  95. Sakaguchi, H., Kadoshima, T., Soen, M., Narii, N., Ishida, Y., Ohgushi, M., Takahashi, J., Eiraku, M., and Sasai, Y. (2015). Generation of functional hippocampal neurons from self-organizing human embryonic stem cell-derived dorsomedial telencephalic tissue. *Nat. Commun.* 6, 8896. <https://doi.org/10.1038/ncomms9896>.
  96. Qian, X., Nguyen, H.N., Song, M.M., Hadiono, C., Ogden, S.C., Hammack, C., Yao, B., Hamersky, G.R., Jacob, F., Zhong, C., et al. (2016). Brain-Region-Specific Organoids Using Mini-bioreactors for Modeling ZIKV Exposure. *Cell* 165, 1238–1254. <https://doi.org/10.1016/j.cell.2016.04.032>.
  97. Shiraishi, A., Muguruma, K., and Sasai, Y. (2017). Generation of thalamic neurons from mouse embryonic stem cells. *Dev* 144, 1211–1220. <https://doi.org/10.1242/dev.144071>.
  98. Xiang, Y., Tanaka, Y., Cakir, B., Patterson, B., Kim, K.Y., Sun, P., Kang, Y.J., Zhong, M., Liu, X., Patra, P., et al. (2019). hESC-Derived Thalamic Organoids Form Reciprocal Projections When Fused with Cortical Organoids. *Cell Stem Cell* 24, 487–497.e7. <https://doi.org/10.1016/j.stem.2018.12.015>.
  99. Phillips, M.J., Wallace, K.A., Dickerson, S.J., Miller, M.J., Verhoeven, A.D., Martin, J.M., Wright, L.S., Shen, W., Capowski, E.E., Percin, E.F., et al. (2012). Blood-derived human iPS cells generate optic vesicle-like structures with the capacity to form retinal laminae and develop synapses. *Invest. Ophthalmol. Vis. Sci.* 53, 2007–2019. <https://doi.org/10.1167/iov.11-9313>.
  100. Nakano, T., Ando, S., Takata, N., Kawada, M., Muguruma, K., Sekiguchi, K., Saito, K., Yonemura, S., Eiraku, M., and Sasai, Y. (2012). Self-formation of optic cups and storable stratified neural retina from human ESCs. *Cell Stem Cell* 10, 771–785. <https://doi.org/10.1016/j.stem.2012.05.009>.
  101. Jo, J., Xiao, Y., Sun, A.X., Cukuroglu, E., Tran, H.D., Göke, J., Tan, Z.Y., Saw, T.Y., Tan, C.P., Lokman, H., et al. (2016). Midbrain-like Organoids from Human Pluripotent Stem Cells Contain Functional Dopaminergic and Neuromelanin-Producing Neurons. *Cell Stem Cell* 19, 248–257. <https://doi.org/10.1016/j.stem.2016.07.005>.
  102. Muguruma, K., Nishiyama, A., Kawakami, H., Hashimoto, K., and Sasai, Y. (2015). Self-organization of polarized cerebellar tissue in 3D culture of human pluripotent stem cells. *Cell Rep.* 10, 537–550. <https://doi.org/10.1016/j.celrep.2014.12.051>.
  103. Eura, N., Matsui, T.K., Luginbühl, J., Matsubayashi, M., Nanaura, H., Shiota, T., Kinugawa, K., Iguchi, N., Kiriya, T., Zheng, C., et al. (2020). Brainstem Organoids From Human Pluripotent Stem Cells. *Front. Neurosci.* 14, 538. <https://doi.org/10.3389/fnins.2020.00538>.
  104. Pellegrini, L., Bonfio, C., Chadwick, J., Begum, F., Skehel, M., and Lancaster, M.A. (2020). Human CNS barrier-forming organoids with

- cerebrospinal fluid production. *Science* 369, eaaz5626. <https://doi.org/10.1126/science.aaz5626>.
105. Ogura, T., Sakaguchi, H., Miyamoto, S., and Takahashi, J. (2018). Three-dimensional induction of dorsal, intermediate and ventral spinal cord tissues from human pluripotent stem cells. *Development* 145, dev162214. <https://doi.org/10.1242/dev.162214>.
  106. Camp, J.G., Badsha, F., Florio, M., Kanton, S., Gerber, T., Wilsch-Bräuninger, M., Lewitus, E., Sykes, A., Hevers, W., Lancaster, M., et al. (2015). Human cerebral organoids recapitulate gene expression programs of fetal neocortex development. *Proc. Natl. Acad. Sci. USA* 112, 15672–15677. <https://doi.org/10.1073/pnas.1520760112>.
  107. Marton, R.M., and Paşca, S.P. (2020). Organoid and Assembloid Technologies for Investigating Cellular Crosstalk in Human Brain Development and Disease. *Trends Cell Biol.* 30, 133–143. <https://doi.org/10.1016/j.tcb.2019.11.004>.
  108. Fedorchak, N.J., Iyer, N., and Ashton, R.S. (2021). Bioengineering tissue morphogenesis and function in human neural organoids. *Semin. Cell Dev. Biol.* 111, 52–59. <https://doi.org/10.1016/j.semcdb.2020.05.025>.
  109. Pham, M.T., Pollock, K.M., Rose, M.D., Cary, W.A., Stewart, H.R., Zhou, P., Nolte, J.A., and Waldau, B. (2018). Generation of human vascularized brain organoids. *Neuroreport* 29, 588–593. <https://doi.org/10.1097/WNR.0000000000001014>.
  110. Cakir, B., Xiang, Y., Tanaka, Y., Kural, M.H., Parent, M., Kang, Y.J., Chappeton, K., Patterson, B., Yuan, Y., He, C.S., et al. (2019). Engineering of human brain organoids with a functional vascular-like system. *Nat. Methods* 16, 1169–1175. <https://doi.org/10.1038/s41592-019-0586-5>.
  111. Lancaster, M.A., Corsini, N.S., Wolfinger, S., Gustafson, E.H., Phillips, A.W., Burkard, T.R., Otani, T., Livesey, F.J., and Knoblich, J.A. (2017). Guided self-organization and cortical plate formation in human brain organoids. *Nat. Biotechnol.* 35, 659–666. <https://doi.org/10.1038/nbt.3906>.
  112. Qian, X., Song, H., and Ming, G.L. (2019). Brain organoids: Advances, applications and challenges. *Development* 146, dev166074. <https://doi.org/10.1242/dev.166074>.
  113. Lancaster, M.A., and Knoblich, J.A. (2014). Generation of cerebral organoids from human pluripotent stem cells. *Nat. Protoc.* 9, 2329–2340. <https://doi.org/10.1038/nprot.2014.158>.
  114. Balikov, D.A., Neal, E.H., and Lippmann, E.S. (2020). Organotypic Neurovascular Models: Past Results and Future Directions. *Trends Mol. Med.* 26, 273–284. <https://doi.org/10.1016/j.molmed.2019.09.010>.
  115. Xu, M., He, J., Zhang, C., Xu, J., and Wang, Y. (2019). Strategies for derivation of endothelial lineages from human stem cells. *Stem Cell Res. Ther.* 10, 200. <https://doi.org/10.1186/s13287-019-1274-1>.
  116. Shi, Y., Sun, L., Wang, M., Liu, J., Zhong, S., Li, R., Li, P., Guo, L., Fang, A., Chen, R., et al. (2020). Vascularized human cortical organoids (vOrganoids) model cortical development in vivo. *PLoS Biol.* 18, e3000705. <https://doi.org/10.1371/journal.pbio.3000705>.
  117. Gomes, A.R., Fernandes, T.G., Vaz, S.H., Silva, T.P., Bekman, E.P., Xapelli, S., Duarte, S., Ghazvini, M., Gribnau, J., Muotri, A.R., et al. (2020). Modeling Rett Syndrome With Human Patient-Specific Forebrain Organoids. *Front. Cell Dev. Biol.* 8, 610427. <https://doi.org/10.3389/fcell.2020.610427>.
  118. Vogenstahl, J., Parrilla, M., Acker-Palmer, A., and Segarra, M. (2022). Vascular Regulation of Developmental Neurogenesis. *Front. Cell Dev. Biol.* 10, 890852. <https://doi.org/10.3389/fcell.2022.890852>.
  119. Sun, X.Y., Ju, X.C., Li, Y., Zeng, P.M., Wu, J., Zhou, Y.Y., Shen, L.B., Dong, J., Chen, Y.J., and Luo, Z.G. (2022). Generation of Vascularized Brain Organoids to Study Neurovascular Interactions. *Elife* 11, e76707. <https://doi.org/10.7554/eLife.76707>.
  120. Wörsdörfer, P., Dalda, N., Kern, A., Krüger, S., Wagner, N., Kwok, C.K., Henke, E., and Ergün, S. (2019). Generation of complex human organoid models including vascular networks by incorporation of mesodermal progenitor cells. *Sci. Rep.* 9, 15663. <https://doi.org/10.1038/s41598-019-52204-7>.
  121. Wörsdörfer, P., Rockel, A., Alt, Y., Kern, A., and Ergün, S. (2020). Generation of Vascularized Neural Organoids by Co-culturing with Mesodermal Progenitor Cells. *STAR Protoc.* 1, 100041. <https://doi.org/10.1016/j.xpro.2020.100041>.
  122. Song, L., Yuan, X., Jones, Z., Griffin, K., Zhou, Y., Ma, T., and Li, Y. (2019). Assembly of Human Stem Cell-Derived Cortical Spheroids and Vascular Spheroids to Model 3-D Brain-like Tissues. *Sci. Rep.* 9, 5977. <https://doi.org/10.1038/s41598-019-42439-9>.
  123. Wang, L., Sievert, D., Clark, A.E., Lee, S., Federman, H., Gastfriend, B.D., Shusta, E.V., Palecek, S.P., Carlin, A.F., and Gleeson, J.G. (2021). A human three-dimensional neural-perivascular “assembloid” promotes astrocytic development and enables modeling of SARS-CoV-2 neuropathology. *Nat. Med.* 27, 1600–1606. <https://doi.org/10.1038/s41591-021-01443-1>.
  124. Dao, L., You, Z., Lu, L., Xu, T., Sarkar, A.K., Zhu, H., Liu, M., Calandrelli, R., Yoshida, G., Lin, P., et al. (2024). Modeling blood-brain barrier formation and cerebral cavernous malformations in human PSC-derived organoids. *Cell Stem Cell* 31, 818–833.e11. <https://doi.org/10.1016/j.stem.2024.04.019>.
  125. Cho, C., Smallwood, P.M., and Nathans, J. (2017). Reck and Gpr124 Are Essential Receptor Cofactors for Wnt7a/Wnt7b-Specific Signaling in Mammalian CNS Angiogenesis and Blood-Brain Barrier Regulation. *Neuron* 95, 1056–1073.e5. <https://doi.org/10.1016/j.neuron.2017.07.031>.
  126. Bonney, S., Harrison-Uy, S., Mishra, S., MacPherson, A.M., Choe, Y., Li, D., Jaminet, S.C., Fruttiger, M., Pleasure, S.J., and Siegenthaler, J.A. (2016). Diverse functions of retinoic acid in brain vascular development. *J. Neurosci.* 36, 7786–7801. <https://doi.org/10.1523/JNEUROSCI.3952-15.2016>.
  127. Ham, O., Jin, Y.B., Kim, J., and Lee, M.O. (2020). Blood vessel formation in cerebral organoids formed from human embryonic stem cells. *Biochem. Biophys. Res. Commun.* 521, 84–90. <https://doi.org/10.1016/j.bbrc.2019.10.079>.
  128. Wang, K., Lin, R.-Z., Hong, X., Ng, A.H., Lee, C.N., Neumeier, J., Wang, G., Wang, X., Ma, M., Pu, W.T., et al. (2020). Robust differentiation of human pluripotent stem cells into endothelial cells via temporal modulation of ETV2 with modified mRNA. *Sci. Adv.* 6, eaba7606. <https://doi.org/10.1126/sciadv.aba7606>.
  129. Palikuqi, B., Nguyen, D.-H.T., Li, G., Schreiner, R., Pellegata, A.F., Liu, Y., Redmond, D., Geng, F., Lin, Y., Gómez-Salineró, J.M., et al. (2020). Adaptable haemodynamic endothelial cells for organogenesis and tumorigenesis. *Nature* 585, 426–432. <https://doi.org/10.1038/s41586-020-2712-z>.
  130. Vargas-Valderrama, A., Messina, A., Mitjavila-Garcia, M.T., and Guenou, H. (2020). The endothelium, a key actor in organ development and hPSC-derived organoid vascularization. *J. Biomed. Sci.* 27, 67. <https://doi.org/10.1186/s12929-020-00661-y>.
  131. Karzbrun, E., Khankhel, A.H., Megale, H.C., Glasauer, S.M.K., Wyle, Y., Britton, G., Warmflash, A., Kosik, K.S., Siggia, E.D., Shraiman, B.I., and Streichan, S.J. (2021). Human neural tube morphogenesis in vitro by geometric constraints. *Nature* 599, 268–272. <https://doi.org/10.1038/s41586-021-04026-9>.
  132. Xue, X., Kim, Y.S., Ponce-Arias, A.I., O’Laughlin, R., Yan, R.Z., Kobayashi, N., Tshuva, R.Y., Tsai, Y.H., Sun, S., Zheng, Y., et al. (2024). A patterned human neural tube model using microfluidic gradients. *Nature* 628, 391–399. <https://doi.org/10.1038/s41586-024-07204-7>.
  133. Lundin, B.F., Knight, G.T., Fedorchak, N.J., Krucki, K., Iyer, N., Maher, J.E., Izban, N.R., Roberts, A., Cicero, M.R., Robinson, J.F., et al. (2024). RosetteArray® Platform for Quantitative High-Throughput Screening of Human Neurodevelopmental Risk. Preprint at: bioRxiv, 2024.04.01.587605. <https://doi.org/10.1101/2024.04.01.587605>

134. Knight, G.T., Lundin, B.F., Iyer, N., Ashton, L.M., Sethares, W.A., Willett, R.M., and Ashton, R.S. (2018). Engineering induction of singular neural rosette emergence within hPSC-derived tissues. *Elife* 7, e37549. <https://doi.org/10.7554/eLife.37549>.
135. Rocha, L.A., Gomes, E.D., Afonso, J.L., Granja, S., Baltazar, F., Silva, N.A., Shoichet, M.S., Sousa, R.A., Learmonth, D.A., and Salgado, A.J. (2020). In vitro Evaluation of ASCs and HUVECs Co-cultures in 3D Biodegradable Hydrogels on Neurite Outgrowth and Vascular Organization. *Front. Cell Dev. Biol.* 8, 489. <https://doi.org/10.3389/fcell.2020.00489>.
136. Miller, J.S., Stevens, K.R., Yang, M.T., Baker, B.M., Nguyen, D.-H.T., Cohen, D.M., Toro, E., Chen, A.A., Galie, P.A., Yu, X., et al. (2012). Rapid casting of patterned vascular networks for perfusable engineered three-dimensional tissues. *Nat. Mater.* 11, 768–774. <https://doi.org/10.1038/nmat3357>.
137. Zhang, S., Wan, Z., and Kamm, R.D. (2021). Vascularized organoids on a chip: Strategies for engineering organoids with functional vasculature. *Lab Chip* 21, 473–488. <https://doi.org/10.1039/d0lc01186j>.
138. Phan, D.T., Bender, R.H.F., Andrejcsk, J.W., Sobrino, A., Hachey, S.J., George, S.C., and Hughes, C.C. (2017). Blood-brain barrier-on-a-chip: Microphysiological systems that capture the complexity of the blood-central nervous system interface. *Exp. Biol. Med.* 242, 1669–1678. <https://doi.org/10.1177/1535370217694100>.
139. Kaushik, G., Gupta, K., Harms, V., Torr, E., Evans, J., Johnson, H.J., Soref, C., Acevedo-Acevedo, S., Antosiewicz-Bourget, J., Mamott, D., et al. (2020). Engineered Perineural Vascular Plexus for Modeling Developmental Toxicity. *Adv. Healthc. Mater.* 9, 2000825. <https://doi.org/10.1002/adhm.202000825>.
140. Daviaud, N., Friedel, R.H., and Zou, H. (2018). Vascularization and engraftment of transplanted human cerebral organoids in mouse cortex. *eNeuro* 5. <https://doi.org/10.1523/ENEURO.0219-18.2018>.
141. Mansour, A.A., Gonçalves, J.T., Bloyd, C.W., Li, H., Fernandes, S., Quang, D., Johnston, S., Parylak, S.L., Jin, X., and Gage, F.H. (2018). An in vivo model of functional and vascularized human brain organoids. *Nat. Biotechnol.* 36, 432–441. <https://doi.org/10.1038/nbt.4127>.
142. Nzou, G., Wicks, R.T., VanOstrand, N.R., Mekky, G.A., Seale, S.A., EL-Taibany, A., Wicks, E.E., Nechtman, C.M., Marrotte, E.J., Makani, V.S., et al. (2020). Multicellular 3D Neurovascular Unit Model for Assessing Hypoxia and Neuroinflammation Induced Blood-Brain Barrier Dysfunction. *Sci. Rep.* 10, 9766. <https://doi.org/10.1038/s41598-020-66487-8>.
143. Blanchard, J.W., Bula, M., Davila-Velderrain, J., Akay, L.A., Zhu, L., Frank, A., Victor, M.B., Bonner, J.M., Mathys, H., Lin, Y.-T., et al. (2020). Reconstruction of the human blood-brain barrier in vitro reveals a pathogenic mechanism of APOE4 in pericytes. *Nat. Med.* 26, 952–963. <https://doi.org/10.1038/s41591-020-0886-4>.
144. Zhao, X., and Bhattacharyya, A. (2018). Human Models Are Needed for Studying Human Neurodevelopmental Disorders. *Am. J. Hum. Genet.* 103, 829–857. <https://doi.org/10.1016/j.ajhg.2018.10.009>.
145. Workman, M.J., and Svendsen, C.N. (2020). Recent advances in human iPSC-derived models of the blood-brain barrier. *Fluids Barriers CNS* 17, 30. <https://doi.org/10.1186/s12987-020-00191-7>.
146. Song, H.W., Foreman, K.L., Gastfriend, B.D., Kuo, J.S., Palecek, S.P., and Shusta, E.V. (2020). Transcriptomic comparison of human and mouse brain microvessels. *Sci. Rep.* 10, 12358. <https://doi.org/10.1038/s41598-020-69096-7>.
147. LaFerla, F.M., and Green, K.N. (2012). Animal Models of Alzheimer's Disease. *Cold Spring Harb. Perspect. Med.* 2, a006320. <https://doi.org/10.1101/cshperspect.a006320>.
148. Trujillo, C.A., Gao, R., Negraes, P.D., Gu, J., Buchanan, J., Preissl, S., Wang, A., Wu, W., Haddad, G.G., Chaim, I.A., et al. (2019). Complex Oscillatory Waves Emerging from Cortical Organoids Model Early Human Brain Network Development. *Cell Stem Cell* 25, 558–569.e7. <https://doi.org/10.1016/j.stem.2019.08.002>.
149. O'Hara-Wright, M., and Gonzalez-Cordero, A. (2020). Retinal organoids: A window into human retinal development. *Development* 147, dev189746. <https://doi.org/10.1242/dev.189746>.
150. Mariani, J., Coppola, G., Zhang, P., Abyzov, A., Provini, L., Tomasini, L., Mariani, J., Coppola, G., Zhang, P., Wilson, M., and Amenduni, M. (2015). FOXG1-Dependent Dysregulation of GABA/Glutamate Neuron Differentiation in Autism. *Cell* 162, 375–390. <https://doi.org/10.1016/j.cell.2015.06.034>.
151. Kim, H., Park, H.J., Choi, H., Chang, Y., Park, H., Shin, J., Kim, J., Lengner, C.J., Lee, Y.K., and Kim, J. (2019). Modeling G2019S-LRRK2 Sporadic Parkinson's Disease in 3D Midbrain Organoids. *Stem Cell Rep.* 12, 518–531. <https://doi.org/10.1016/j.stemcr.2019.01.020>.
152. Wegscheid, M.L., Anastasaki, C., Hartigan, K.A., Cobb, O.M., Papke, J.B., Traber, J.N., Morris, S.M., and Gutmann, D.H. (2021). Patient-derived iPSC-cerebral organoid modeling of the 17q11.2 microdeletion syndrome establishes CRLF3 as a critical regulator of neurogenesis. *Cell Rep.* 36, 109315. <https://doi.org/10.1016/j.celrep.2021.109315>.
153. Chen, X., Sun, G., Tian, E., Zhang, M., Davtyan, H., Beach, T.G., Reiman, E.M., Blurton-Jones, M., Holtzman, D.M., and Shi, Y. (2021). Modeling Sporadic Alzheimer's Disease in Human Brain Organoids under Serum Exposure. *Adv. Sci.* 8, e2101462. <https://doi.org/10.1002/adv.202101462>.
154. Wang, S.N., Wang, Z., Xu, T.Y., Cheng, M.H., Li, W.L., and Miao, C.Y. (2020). Cerebral Organoids Repair Ischemic Stroke Brain Injury. *Transl. Stroke Res.* 11, 983–1000. <https://doi.org/10.1007/s12975-019-00773-0>.
155. Biswas, S., Cottarelli, A., and Agalliu, D. (2020). Neuronal and glial regulation of CNS angiogenesis and barrierogenesis. *Development* 147, dev182279. <https://doi.org/10.1242/dev.182279>.
156. Miyamoto, N., Pham, L.D.D., Seo, J.H., Kim, K.W., Lo, E.H., and Arai, K. (2014). Crosstalk between cerebral endothelium and oligodendrocyte. *Cell. Mol. Life Sci.* 71, 1055–1066. <https://doi.org/10.1007/s00018-013-1488-9>.
157. Quadrato, G., Nguyen, T., Macosko, E.Z., Sherwood, J.L., Min Yang, S., Berger, D.R., Maria, N., Scholvin, J., Goldman, M., Kinney, J.P., et al. (2017). Cell diversity and network dynamics in photosensitive human brain organoids. *Nature* 545, 48–53. <https://doi.org/10.1038/nature22047>.
158. Marton, R.M., Miura, Y., Sloan, S.A., Li, Q., Revah, O., Levy, R.J., Huguenard, J.R., and Paşca, S.P. (2019). Differentiation and maturation of oligodendrocytes in human three-dimensional neural cultures. *Nat. Neurosci.* 22, 484–491. <https://doi.org/10.1038/s41593-018-0316-9>.
159. Qian, X., Su, Y., Adam, C.D., Deutschmann, A.U., Pather, S.R., Goldberg, E.M., Su, K., Li, S., Lu, L., Jacob, F., et al. (2020). Sliced Human Cortical Organoids for Modeling Distinct Cortical Layer Formation. *Cell Stem Cell* 26, 766–781.e9. <https://doi.org/10.1016/j.stem.2020.02.002>.
160. Madhavan, M., Nevin, Z.S., Shick, H.E., Garrison, E., Clarkson-Paredes, C., Karl, M., Clayton, B.L.L., Factor, D.C., Allan, K.C., Barbar, L., et al. (2018). Induction of myelinating oligodendrocytes in human cortical spheroids. *Nat. Methods* 15, 700–706. <https://doi.org/10.1038/s41592-018-0081-4>.
161. Kim, H., Xu, R., Padmashri, R., Dunaevsky, A., Liu, Y., Dreyfus, C.F., and Jiang, P. (2019). Pluripotent Stem Cell-Derived Cerebral Organoids Reveal Human Oligodendrogenesis with Dorsal and Ventral Origins. *Stem Cell Rep.* 12, 890–905. <https://doi.org/10.1016/j.stemcr.2019.04.011>.
162. Ortiz, G.G., Pacheco-Moisés, F.P., Macías-Islas, M.Á., Flores-Alvarado, L.J., Mireles-Ramírez, M.A., González-Renovato, E.D., Hernández-Navarro, V.E., Sánchez-López, A.L., and Alatorre-Jiménez, M.A. (2014). Role of the Blood-Brain Barrier in Multiple Sclerosis. *Arch. Med. Res.* 45, 687–697. <https://doi.org/10.1016/j.arcmed.2014.11.013>.
163. Jiang, X., Anđjelkovic, A.V., Zhu, L., Yang, T., Bennett, M.V.L., Chen, J., Keep, R.F., and Shi, Y. (2018). Blood-brain barrier dysfunction and recovery after ischemic stroke. *Prog. Neurobiol.* 163–164, 144–171. <https://doi.org/10.1016/j.pneurobio.2017.10.001>.

164. Cai, Z., Qiao, P.F., Wan, C.Q., Cai, M., Zhou, N.K., and Li, Q. (2018). Role of Blood-Brain Barrier in Alzheimer's Disease. *J. Alzheimer's Dis.* 63, 1223–1234. <https://doi.org/10.3233/JAD-180098>.
165. Drouin-Ouellet, J., Sawiak, S.J., Cisbani, G., Lagacé, M., Kuan, W.L., Saint-Pierre, M., Dury, R.J., Alata, W., St-Amour, I., Mason, S.L., et al. (2015). Cerebrovascular and blood-brain barrier impairments in Huntington's disease: Potential implications for its pathophysiology. *Ann. Neurol.* 78, 160–177. <https://doi.org/10.1002/ana.24406>.
166. Paul, G., and Elabi, O.F. (2022). Microvascular Changes in Parkinson's Disease- Focus on the Neurovascular Unit. *Front. Aging Neurosci.* 14, 853372. <https://doi.org/10.3389/fnagi.2022.853372>.
167. Wolburg, H., Noell, S., Fallier-Becker, P., MacK, A.F., and Wolburg-Buchholz, K. (2012). The disturbed blood-brain barrier in human glioblastoma. *Mol. Aspects Med.* 33, 579–589. <https://doi.org/10.1016/j.mam.2012.02.003>.
168. Nishihara, H., Perriot, S., Gastfriend, B.D., Steinfert, M., Cibien, C., Soldati, S., Matsuo, K., Guimbal, S., Mathias, A., Palecek, S.P., et al. (2022). Intrinsic blood-brain barrier dysfunction contributes to multiple sclerosis pathogenesis. *Brain* 145, 4334–4348. <https://doi.org/10.1093/brain/awac019>.
169. Winkler, E.A., Birk, H., Burkhardt, J.K., Chen, X., Yue, J.K., Guo, D., Rutledge, W.C., Lasker, G.F., Partow, C., Tihan, T., et al. (2018). Reductions in brain pericytes are associated with arteriovenous malformation vascular instability. *J. Neurosurg.* 129, 1464–1474. <https://doi.org/10.3171/2017.6.JNS17860>.
170. Dai, C., Xiao, J., Wang, C., Li, W., and Su, G. (2022). Neurovascular abnormalities in retinopathy of prematurity and emerging therapies. *J. Mol. Med.* 100, 817–828. <https://doi.org/10.1007/s00109-022-02195-2>.
171. Hudson, N., Celkova, L., Hopkins, A., Greene, C., Storti, F., Ozaki, E., Fahy, E., Theodoropoulou, S., Kenna, P.F., Humphries, M.M., et al. (2019). Dysregulated claudin-5 cycling in the inner retina causes retinal pigment epithelial cell atrophy. *JCI Insight* 4, e130273. <https://doi.org/10.1172/jci.insight.130273>.
172. Greene, C., Hanley, N., and Campbell, M. (2020). Blood-brain barrier associated tight junction disruption is a hallmark feature of major psychiatric disorders. *Transl. Psychiatry* 10, 373. <https://doi.org/10.1038/s41398-020-01054-3>.
173. Kim, K.R., Jung, S.W., and Kim, D.W. (2014). Risk factors associated with germinal matrix-intraventricular hemorrhage in preterm neonates. *J. Korean Neurosurg. Soc.* 56, 334–337. <https://doi.org/10.3340/jkns.2014.56.4.334>.
174. Williams, K.P., Fields, M.E., Ragan, D.K., Chen, Y., Eldeniz, C., Hulbert, M.L., Binkley, M.M., Rhodes, J.N., Shimony, J.S., McKinstry, R.C., et al. (2017). Large Vessel Vasculopathy in Children with Sickle Cell Disease: an MRI study of Infarct Topography and Focal Atrophy. *Pediatr. Neurol.* 69, 49–57. <https://doi.org/10.1016/j.pediatrneurol.2016.11.005>.
175. Sharma, K., Krohne, T.U., and Buskamp, V. (2020). The rise of retinal organoids for vision research. *Int. J. Mol. Sci.* 21, 8484. <https://doi.org/10.3390/ijms21228484>.
176. Merkle, F.T., and Eggen, K. (2013). Modeling human disease with pluripotent stem cells: From genome association to function. *Cell Stem Cell* 12, 656–668. <https://doi.org/10.1016/j.stem.2013.05.016>.
177. Moon, W.J., Lim, C., Ha, I.H., Kim, Y., Moon, Y., Kim, H.J., and Han, S.H. (2021). Hippocampal blood-brain barrier permeability is related to the APOE4 mutation status of elderly individuals without dementia. *J. Cereb. Blood Flow Metab.* 41, 1351–1361. <https://doi.org/10.1177/0271678X20952012>.
178. Zhang, X., Yin, X., Zhang, J., Li, A., Gong, H., Luo, Q., Zhang, H., Gao, Z., and Jiang, H. (2019). High-resolution mapping of brain vasculature and its impairment in the hippocampus of Alzheimer's disease mice. *Natl. Sci. Rev.* 6, 1223–1238. <https://doi.org/10.1093/nsr/nwz124>.
179. Luo, C., Lancaster, M.A., Castanon, R., Nery, J.R., Knoblich, J.A., and Ecker, J.R. (2016). Cerebral Organoids Recapitulate Epigenomic Signatures of the Human Fetal Brain. *Cell Rep.* 17, 3369–3384. <https://doi.org/10.1016/j.celrep.2016.12.001>.
180. Grenier, K., Kao, J., and Diamandis, P. (2020). Three-dimensional modeling of human neurodegeneration: brain organoids coming of age. *Mol. Psychiatry* 25, 254–274. <https://doi.org/10.1038/s41380-019-0500-7>.
181. Shen, Q., Goderie, S.K., Jin, L., Karanth, N., Sun, Y., Abramova, N., Vincent, P., Pumiglia, K., and Temple, S. (2004). Endothelial cells stimulate self-renewal and expand neurogenesis of neural stem cells. *Science* 304, 1338–1340. <https://doi.org/10.1126/science.1095505>.
182. Shen, Q., Wang, Y., Kokovay, E., Lin, G., Chuang, S.M., Goderie, S.K., Roysam, B., and Temple, S. (2008). Adult SVZ Stem Cells Lie in a Vascular Niche: A Quantitative Analysis of Niche Cell-Cell Interactions. *Cell Stem Cell* 3, 289–300. <https://doi.org/10.1016/j.stem.2008.07.026>.
183. Wimmer, R.A., Leopoldi, A., Aichinger, M., Wick, N., Hantusch, B., Novatchkova, M., Taubenschmid, J., Hämmerle, M., Esk, C., Bagley, J.A., et al. (2019). Human blood vessel organoids as a model of diabetic vasculopathy. *Nature* 565, 505–510. <https://doi.org/10.1038/s41586-018-0858-8>.
184. Marti-Figueroa, C.R., and Ashton, R.S. (2017). The case for applying tissue engineering methodologies to instruct human organoid morphogenesis. *Acta Biomater.* 54, 35–44. <https://doi.org/10.1016/j.actbio.2017.03.023>.
185. Justin, A.W., Brooks, R.A., and Markaki, A.E. (2016). Multi-casting approach for vascular networks in cellularized hydrogels. *J. R. Soc. Interface* 13, 20160768. <https://doi.org/10.1098/rsif.2016.0768>.
186. McNulty, J.D., Marti-Figueroa, C., Seipel, F., Plantz, J.Z., Ellingham, T., Duddlestone, L.J.L., Goris, S., Cox, B.L., Osswald, T.A., Turng, L.-S., and Ashton, R.S. (2019). Micro-injection molded, poly(vinyl alcohol)-calcium salt templates for precise customization of 3D hydrogel internal architecture. *Acta Biomater.* 95, 258–268. <https://doi.org/10.1016/j.actbio.2019.04.050>.
187. Grigoryan, B., Paulsen, S.J., Corbett, D.C., Sazer, D.W., Fortin, C.L., Zaita, A.J., Greenfield, P.T., Calafat, N.J., Gounley, J.P., Ta, A.H., et al. (2019). Multivascular networks and functional intravascular topologies within biocompatible hydrogels. *Science* 364, 458–464. <https://doi.org/10.1126/science.aav9750>.
188. Hinton, T.J., Jallerat, Q., Palchesko, R.N., Park, J.H., Grodzicki, M.S., Shue, H.-J., Ramadan, M.H., Hudson, A.R., and Feinberg, A.W. (2015). Three-dimensional printing of complex biological structures by freeform reversible embedding of suspended hydrogels. *Sci. Adv.* 1, e1500758. <https://doi.org/10.1126/sciadv.1500758>.
189. Mirdamadi, E., Tashman, J.W., Shiwarski, D.J., Palchesko, R.N., and Feinberg, A.W. (2020). FRESH 3D Bioprinting a Full-Size Model of the Human Heart. *ACS Biomater. Sci. Eng.* 6, 6453–6459. <https://doi.org/10.1021/acsbomaterials.0c01133>.
190. Pascoal, J.F., Fernandes, T.G., Nierode, G.J., Diogo, M.M., Dordick, J.S., and Cabral, J.M.S. (2018). Three-Dimensional Cell-Based Microarrays: Printing Pluripotent Stem Cells into 3D Microenvironments. In *Methods in Molecular Biology*, Springer pp. 69–81. [https://doi.org/10.1007/978-1-4939-7792-5\\_6](https://doi.org/10.1007/978-1-4939-7792-5_6).
191. Skylar-Scott, M.A., Uzel, S.G.M., Nam, L.L., Ahrens, J.H., Truby, R.L., Damaraju, S., and Lewis, J.A. (2019). Biomanufacturing of organ-specific tissues with high cellular density and embedded vascular channels. *Sci. Adv.* 5, eaaw2459. <https://doi.org/10.1126/sciadv.aaw2459>.